Published online 12 December 2019

Nucleic Acids Research, 2020, Vol. 48, No. 4 ***1627–1651***
doi: 10.1093/nar/gkz1140

SURVEY AND SUMMARY

Functional diversity of small nucleolar RNAs

Tomaž Bratkovič [1,*], Janja Božič [2,3] and Boris Rogelj [1,2,3,4,*]

[1]University of Ljubljana, Faculty of Pharmacy, Aškerčeva cesta 7, SI1000 Ljubljana, Slovenia, [2]Jozef Stefan Institute, Department of Biotechnology, Jamova cesta 39, SI1000 Ljubljana, Slovenia, [3]Biomedical Research Institute BRIS, Puhova ulica 10, SI1000 Ljubljana, Slovenia and [4]University of Ljubljana, Faculty of Chemistry and Chemical Technology, Večna pot 113, SI1000 Ljubljana, Slovenia

Received October 04, 2019; Revised November 17, 2019; Editorial Decision November 20, 2019; Accepted December 05, 2019

ABSTRACT

Small nucleolar RNAs (snoRNAs) are short non-protein-coding RNAs with a long-recognized role in tuning ribosomal and spliceosomal function by guiding ribose methylation and pseudouridylation at targeted nucleotide residues of ribosomal and small nuclear RNAs, respectively. SnoRNAs are increasingly being implicated in regulation of new types of post-transcriptional processes, for example rRNA acetylation, modulation of splicing patterns, control of mRNA abundance and translational efficiency, or they themselves are processed to shorter stable RNA species that seem to be the principal or alternative bioactive isoform. Intriguingly, some display unusual cellular localization under exogenous stimuli, or tissue-specific distribution. Here, we discuss the new and unforeseen roles attributed to snoRNAs, focusing on the presumed mechanisms of action. Furthermore, we review the experimental approaches to study snoRNA function, including high resolution RNA:protein and RNA:RNA interaction mapping, techniques for analyzing modifications on targeted RNAs, and cellular and animal models used in snoRNA biology research.

INTRODUCTION

Small nucleolar RNAs (snoRNAs) constitute a family of short non-protein-coding RNAs (ncRNAs) enriched in the nucleolus and best known for guiding posttranscriptional modifications on ribosomal (rRNAs) and small nuclear RNAs (snRNAs). In yeast, snoRNAs are almost exclusively transcribed from independent promoters, as are the majority of plant snoRNAs. In animals (nematodes, flies, and mammals), however, snoRNAs are mostly embedded in introns, typically following the 'one-gene-per-intron' rule. Plant snoRNA genes display predominate organization in polycistronic clusters, a feature also observed (albeit to a much lesser extent) in yeast and *Drosophila* (1). Based on the characteristic nucleotide motifs and association with canonical partner proteins, snoRNAs are classified into either C/D- (SNORD) or H/ACA-box (SNORA) subfamilies (2–4). C/D-box snoRNAs harbor the C (RUGAUGA, where R is a purine base) and D (CUGA) short sequence motifs that are brought in close proximity through the formation of terminal stem structure, ultimately forming the kink-turn structural element (Figure 1A) (3,5). Most C/D-box snoRNAs contain an additional pair of often less conserved C and D boxes, denoted C′ and D′, respectively. This class of snoRNAs base pairs with target RNAs through a short (7–21 nucleotide) antisense element (ASE; also called guide region) located upstream of the D and/or D′ boxes (Figure 1A). The characteristic C/D-box snoRNA fold attracts partner proteins (primarily Snu13 (formerly called 15.5K or NHP2L1), Nop56, Nop58 and the methyltransferase fibrillarin) and positions them within the snoRNA ribonucleoprotein complex (snoRNP). The partner proteins protect snoRNA from degradation by exonucleases, thereby specifying its 5′- and 3′-ends, and are required for nucleolar localization. Fibrillarin catalyzes the site-specific transfer of methyl group from *S*-adenosylmethionine to the target RNA ribose 2′-hydroxyl group at the nucleotide facing the fifth base counted upstream of the D and/or D' box motif (Figure 1). Based on structural studies of archaeal homologues, C/D-box snoRNPs seem to exist either as monomer assemblies (containing a single snoRNA along with two copies of each protein partner (or the Nop56/Nop58 homologue heterodimer); Figure 1A) or dimer assemblies (containing double amount of each subunit; Figure 1B) (6). It should be noted, though, that *in vitro*, SNU13 was found to only bind to the structural motif formed by C- and D-boxes (as opposed to the

*To whom correspondence should be addressed. Tel: +386 1 4769 570, Fax: +386 1 4258 031; Email: tomaz.bratkovic@ffa.uni-lj.si
Correspondence may also be addressed to Boris Rogelj. Tel: +386 1 4773 611; Fax: +386 1 4773 594; Email: boris.rogelj@ijs.si

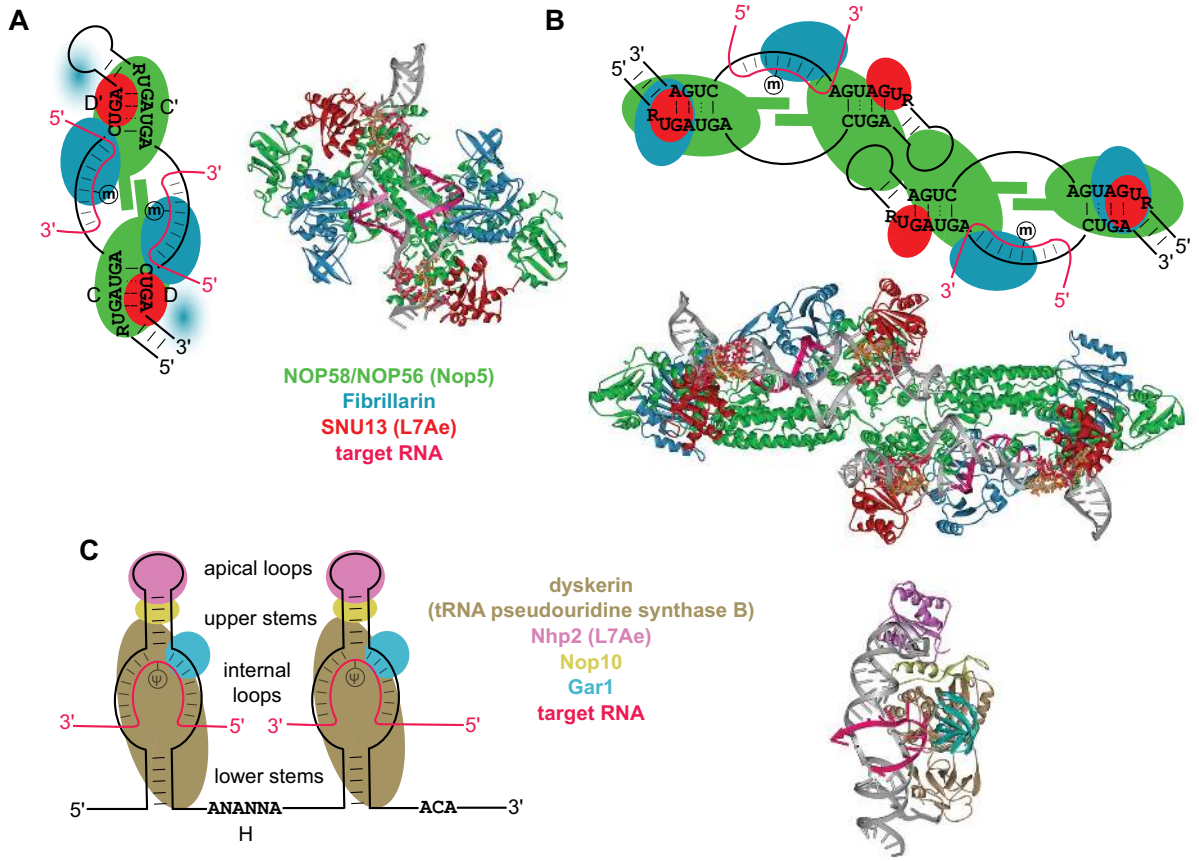

Figure 1. Structures of canonical C/D-box and H/ACA-box snoRNPs, and the modes of target RNA recognition (adapted from (6)). The monomer assembly (**A**) and dimer assembly forms of C/D-box s(no)RNP (**B**). Blurred ovals depict alternative positions of fibrillarins within the monomer architecture. (**C**) Schematic depiction of H/ACA-box snoRNP. Subunit color coding according to the legends in A and C (archeal orthologes of human proteins in parenthesis). Structural models were drawn with ViewerLite (Accelrys): *Saccharolobus solfataricus* C/D RNPs (**A**: PDB ID 5GIO (13); **B:** ID 3PLA (14)) and *Pyrococcus furiosus* H/ACA RNP (**C:** ID 3HAY (15)). SnoRNAs are depicted in gray with C/C'- and D/D'-boxes in dark red and orange, respectively.

C'/D'-box motif) (7), suggesting the presence of a single SNU13 protein within the monomeric C/D-snoRNP assembly. SnoRNAs of the H/ACA-box subfamily fold into two hairpins with internal loops connected by a hinge region harboring the H motif (ANANNA, where N denotes any nucleotide), and contain the ACA box within a short 3′ tail (Figure 1C) (3). The H/ACA-box snoRNAs' antisense region composed of two short nucleotide stretches (9–16 nt combined) is located in the internal loops of 5′ and/or 3′ hairpins (8). Upon base pairing with the target RNA, the uridine residue located opposite the 14th or 15th nucleotide upstream of the H and/or ACA box motifs bulges out into the pseudouridylation pocket of partner uridine isomerase dyskerin. As with C/D-box snoRNAs, H/ACA-box partner proteins (dyskerin, Nhp2, Nop10 and Gar1) are essential for snoRNA biogenesis and stability, and the localization of snoRNPs. Modifications exerted by snoRNPs on the targeted RNAs are believed to convey protection against nucleolytic degradation as well as expand the chemical space of RNA:RNA and RNA:protein interactions (9–12), in turn affecting ribosome and spliceosome function.

A subgroup of C/D-box snoRNAs (e.g. SNORD3, -14, -22 and -118) and SNORA73 are transcribed from independent promoters, and act as co-transcriptional molecular chaperones, regulating excision of rRNAs from the precursor transcript (4,16–19). In contrast to most snoRNAs, they are essential for cell viability. Furthermore, they themselves are processed in a different manner compared to 'conventional' snoRNAs; they lack terminal trimming and associate with additional or alternative partner proteins. Another distinct subfamily of snoRNAs, known as small Cajal body (CB)-specific RNAs (scaRNAs), guide spliceosomal snRNA 2′-*O*-ribose methylation and pseudouridylation in the subnuclear Cajal bodies, and have structural features characteristic to either C/D- or H/ACA-box snoRNAs or both (9). ScaRNAs harbor additional nucleotide motifs (CAB boxes (UGAG) or GU repeats bound by protein Wdr79) required for proper localization. Interestingly, recent findings call for a revision of scaRNA roles as their nuclear localization is not strictly restricted to CBs nor are CBs required for their function (20). Furthermore, they were found not to act exclusively on snRNAs. For a more detailed discussion on canonical snoRNA structures and functions, the reader is referred to past papers (2–4).

In recent years, some snoRNAs have been found to associate with non-canonical protein partners and exhibit unusual cellular localization (e.g. (21–24)), strongly implying alternative or additional roles for this class of ncR-

NAs. In addition, inconsistent with their canonical role in rRNA and snRNA modification is the notion that many of the snoRNAs do not display significant ASE sequence complementarity to canonical targets (thus being termed 'orphan'), and are expressed in a tissue-specific manner (4,25,26). Bioinformatic genome-wide searches suggest that there might still be many snoRNA and snoRNA-like genes currently not annotated in genomic/transcriptomic databases (4,27–29). Some snoRNAs are expressed at lower levels and are less evolutionarily conserved. In the following sections, we provide an overview of unexpected functions attributed to snoRNAs from recent studies.

EMERGING ROLES FOR SNORNA

SnoRNA-guided rRNA acetylation

RNA molecules experience a large variety of post-transcriptional modifications (over 150 with various frequencies have been described) in addition to pseudouridylation and ribose methylation (30–32). However, most modifications are believed to be imposed by stand-alone enzymes (i.e. no guiding RNA specifying the nucleotide to be modified via base pairing to target RNA is required). Eukaryotic 18S rRNA contains two N^4-acetylcytidines (C1280 and C1773 in yeast), located at sites known to determine ribosome information decoding and translation fidelity. Sharma *et al.* (22) used the cross-linking and analysis of cDNAs (CRAC; an advanced RNA immunoprecipitation technique utilizing cross-linking RNA to proteins; see the *SnoRNA:protein interaction screening* section below) to get insights into factors guiding RNA acetylation in yeast. RNA cytidine acetyltransferase Kre33 (an ortholog of human NAT10) chiefly cross-linked to rRNAs and tRNAs, however, unexpected cross-linking to two orphan snoRNAs of the C/D-box subfamily (snR4 and snR45) was also detected. Detailed inspection of snR4 and snR45 sequences revealed extensive bipartite complementarity to regions surrounding the acetylated cytidines on 18S rRNA (Figure 2A). The unusual rRNA:snoRNA interactions (requiring assistance by a Kre33 helicase domain for annealing) suggests that snR4 and snR45 exploit a *modus operandi* similar to that characteristic of H/ACA-box snoRNAs for bulging out the nucleotide to be modified (Figure 2A). Experiments with snR4 and snR45 knock-out strains and those harboring mutated snR4 and snR45 confirmed the role of these snoRNAs in selectively guiding rRNA cytidine acetylation as the extent of rRNA modification was significantly reduced, while no effects on tRNA acetylation were observed. Of note, direct snR45:18S rRNA and snR4:18S rRNA interactions were recently detected by the CLASH method (33) in yeast, and the interaction of SNORD13 (the vertebrate orthologue of snR45) with 18S rRNA was confirmed by the unbiased RNA interactome probing technique PARIS (34) (Figure 2B; see the *RNA:RNA interaction mapping* section below). SNORD13 and snR45 display sequence conservation at the 5′ regions up to the C-box, the internal 18S rRNA binding sites, and the D-box; however, there is poor conservation of regions immediately upstream of the D-box, typically harboring the antisense element in canonical C/D-box snoRNAs (Figure 2C).

SnoRNA-guided tRNA methylation

tRNAs undergo extensive post-transcriptional modifications (36) with rich diversity especially on wobble position 34 of the anticodon and at position 37 located 3′ adjacent to the anticodon triplet, indicating their importance for stabilization of tRNA:mRNA interactions during decoding. In archaea, C/D-box sRNPs perform 2′-*O*-ribose methylation of tRNAs in addition to rRNAs (37), whereas in eukaryotes tRNA post-transcriptional modifications are generated by stand-alone enzymes. A recent study, however, challenges this view. Vitali and Kiss (38) have noted that homologous human orphan snoRNAs SNORD97 and SCARNA97 (previously called SNORD133) display considerable sequence complementarity of the D-box-adjacent antisense element with the anticodon loop of the elongator $tRNA^{Met}$. Assuming that the two orphan snoRNAs obey 'canonical' rules for guiding 2′-*O*-methylation, the wobble cytidine 34 was predicted to be the targeted nucleotide. Indeed, C34 is known to be methylated in vertebrates. Moreover, SNORD97 and SCARNA97 homologues have been identified in all examined vertebrate genomes, while invertebrates (i.e., insects and tunicates) and plants seem to harbor a single SNORD97/SCARNA97 homologue, further implying an evolutionarily highly conserved, yet unexpected function for these snoRNAs. The authors used a human cell line model HAP1 to knock out either one or both homologous snoRNA genes, and (via reintroduction of ectopically expressed snoRNAs) demonstrated that SNORD97 and SCARNA97 work cooperatively to methylate $tRNA^{Met}$ C34. This modification, in turn, was shown to protect the tRNA from cleavage by angiogenin, a stress-induced endonuclease. Notably, no proliferation deficiency was observed in either the single or the double knock-outs, suggesting that wobble nucleotide C34 methylation is not essential for maintaining decoding fidelity as previously presumed, but rather prevents the release of stable 3′ tRNA fragments, important mediators of stress signaling (39,40). It would be interesting to comparatively analyze tRNA fragment-dependent downstream effects of cell stress in wild-type and SNORD97/SCARNA97 knockout cells. Returning to the SNORD97/SCARNA97-snoRNP activity, it remains unclear how the two RNPs accomplish $tRNA^{Met}$ C34 methylation since they localize to nucleolus and CBs, respectively. One possible explanation would be that SNORD97/SCARNA97 are also present in the nucleoplasm, albeit to a small extent, thereby gaining access to the target tRNA (38). Such a hypothesis is corroborated by the notion that CBs are not necessary for the function of scaRNPs (20).

Indirect evidence for snoRNP involvement in eukaryotic tRNA modification comes from earlier studies. While sequencing a cDNA library constructed from RNA, immunoprecipitated with anti-GAR1 antibody, Kiss *et al.* (8) observed a small fraction (<2%) of reads mapping to RNA species other than H/ACA-box snoRNAs and rRNAs, including tRNA and mRNA sequences. Of course, considering tRNA abundance, these might simply be interpreted as non-specifically retained (background) RNAs. Interestingly, tRNAs consistently cross-link to snoRNP protein subunits in CLIP experiments ((41); see the *snoRNA:protein*

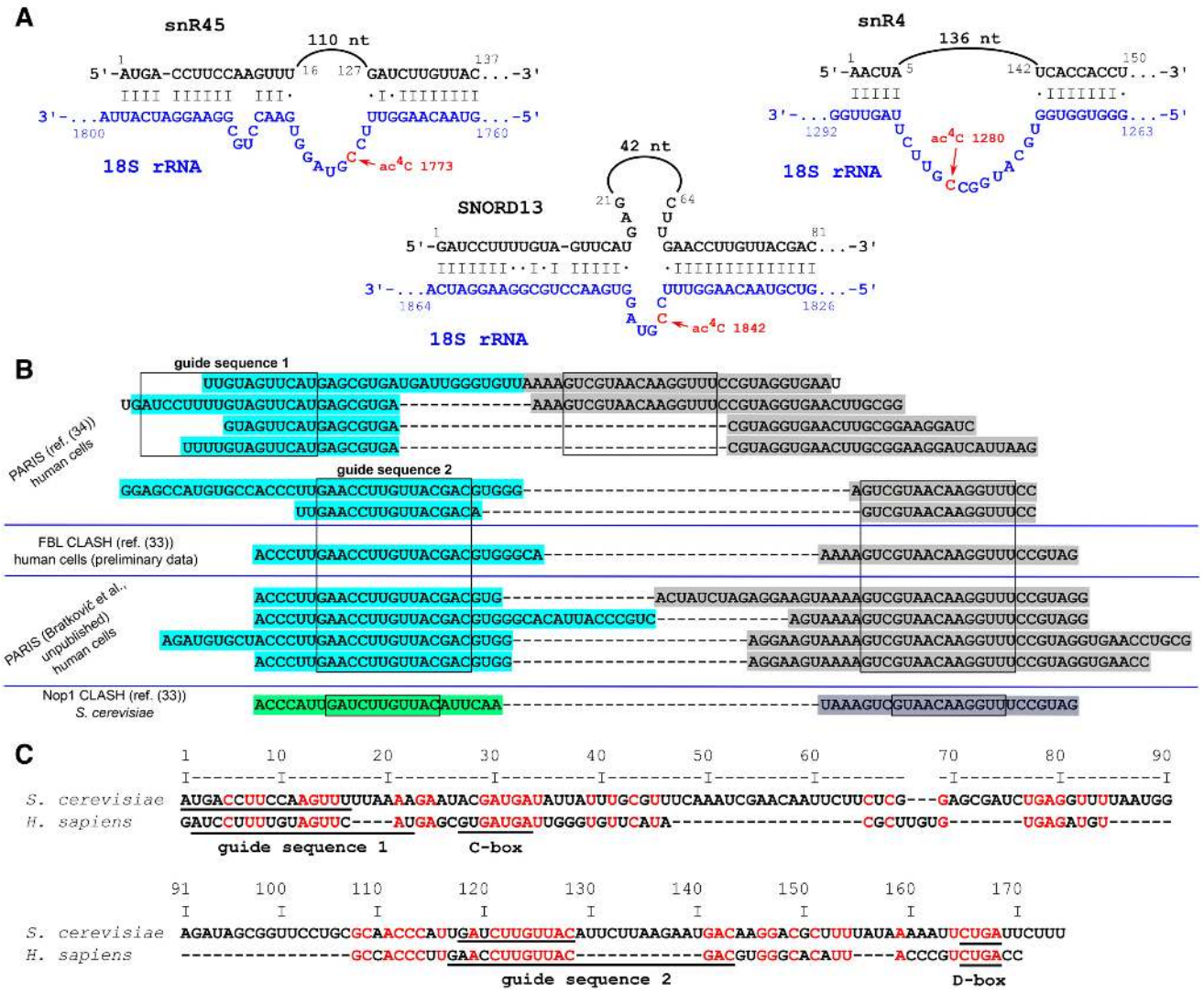

Figure 2. SnR45, snR4 and SNORD13 guide cytidine acetylation in 18S rRNA. (**A**) Proposed interactions of snR45, snR4 and SNORD13 with 18S rRNA (adopted from (22) and (35)). Cytidine targeted for acetylation is shown in red. Watson-Crick base-pairs are denoted by I, G-U base-pairings are denoted by dots. (**B**) Examples of hybrid reads from CLASH (33) and PARIS (34) experiments, confirming the interactions of snR45 or its human orthologue SNORD13 with 18S rRNA. SNORD13 and snR45 fragments are depicted cyan and green, respectively, and 18S rRNA fragments are shown in grey. Interacting sequences are boxed. FBL – fibrillarin, Nop1 – yeast orthologue of FBL. (**C**) Aligned sequences of *Saccharomyces cerevisiae* snR45 and human SNORD13 (adopted from (33)). Numbering according to yeast snR45. The conserved nucleotides are shown in red. Note the unusually long functional 5′ sequence preceding the C-box.

interaction screening section below). Last but not least, Zemann *et al.* (42) have identified 6 potential tRNA targets of previously uncharacterized *Caenorhabditis elegans* snoRNAs in a bioinformatic screening campaign. The snoRNAs presumably target nucleotides at various positions within tRNAs, including the anticodon loop, but their biological effect warrants experimental confirmation.

Regulation of mRNA abundance by snoRNAs

The mechanisms by which snoRNAs affect mRNA abundance seem to be diverse. Huang *et al.* (23) sequenced RNAs associating with mRNA 3′ processing complex (a macromolecular complex of ∼85 proteins) to identify potential trans-acting RNAs involved in gene expression. mRNA 3′ processing can have a decisive effect on transcript turnover, translation efficiency, and cellular mRNA trafficking (43). Unexpectedly, the vast majority of RNAs co-purified with the 3′ mRNA processing complex were snoRNAs (23). By using the iCLIP technique (see the *snoRNA:protein interaction screening* section below), the snoRNA hits were confirmed to selectively interact with FIP1, a component of cleavage and polyadenylation specificity factor (CPSF). One of the highly enriched snoRNAs, SNORD50A, was demonstrated to block FIP1 interaction with a model polyadenylation sequence (belonging to SV40 late gene). Furthermore, comparison of gene expression between wild-type and SNORD50A-depleted HeLa cells revealed significant changes in transcript abundance and alternative polyadenylation profiles for a subset of genes (with 1290

and 878 genes being up- and down-regulated, respectively, by at least 2-fold, and 157 transcripts displaying changes in polyadenylation). Notably, highly upregulated genes were those functioning in cell stress, proliferation, and apoptosis. With regards to the mechanism by which snoRNAs regulate 3′ processing of a subset of mRNAs, the authors propose three possibilities that are not mutually exclusive (44): (i) certain snoRNAs may inhibit mRNA 3′ processing (as indeed is the case for U/A-rich SNORD50A binding to FIP1, thereby likely competing with U-rich sequence adjacent to the mRNA polyadenylation signal of SV40 late gene); (ii) some snoRNAs might in fact promote mRNA 3′ processing complex assembly on non-canonical polyadenylation signals via RNA:RNA interactions or (iii) yet another set of CPSF-associated snoRNAs might stabilize the 3′ processing complex in binding to diverse polyadenylation sites by facilitating protein:RNA or protein:protein interactions. Given that snoRNAs (including SNORD50A) are often deregulated in cancers (45,46), it is tempting to speculate that they play a causative role in cancer development and progression by affecting oncogene and/or tumor suppressor gene expression via mRNA processing. Looking at bigger picture, mRNA 3′ processing dysregulation may well promote the bicistronic transcription of downstream genes, adding another layer of complexity to potential snoRNA effects on gene expression (44).

Orphan brain-specific snoRNAs SNORD115 and SNORD116 have attracted attention of neuroscientists as they reside in an imprinted region of chromosome 15 whose deletion is believed to be responsible for the complex neurodevelopmental disorder called the Prader-Willi syndrome (PWS; see the *SnoRNAs implicated in Prader-Willi syndrome* section below). Falaleeva *et al.* (47) ectopically expressed SNORD116 either alone or in combination with SNORD115 in HEK293T cells, and monitored gene expression changes using exon junction microarrays. Overexpression of SNORD116 affected the levels of 274 genes, whereas coexpression of SNORD115 affected expression of 415 genes; most changes involved gene upregulation. Although microarray analyses also suggested subtle changes in alternative exon usage for several transcripts, none could be validated by RT-PCR. Interestingly, only limited overlap of gene expression changes was observed between experiments in which SNORD116 was overexpressed separately or together with SNORD115, suggesting that SNORD115 can modify the action of SNORD116 on transcript abundance. Finally, authors confirmed that 23 hits from the *in vitro* experiment overlapped with genes that display dysregulated expression in brains of PWS subjects ($P = 0.00735$, chi-squared test). It remains unclear whether the snoRNAs exert the observed effects on mRNA abundance directly or indirectly by regulating a trans-acting factor. Assuming that SNORD115 and SNORD116 are involved in RNA:RNA interactions similarly as the canonical snoRNAs, recent methods allowing RNA interactome mapping in live cells (see the *RNA:RNA interaction mapping* section below) may provide the answer to such questions. For example, by applying the LIGR-seq technique on HEK293T cells, Sharma *et al.* (48) identified several mRNA targets of orphan SNORD83B (Figure 3). When SNORD83B was depleted by two different RNase H-recruiting antisense oligonucleotides (ASOs), the steady state levels of SNORD83B-targeted NOP14, RPS5, and SRSF3 mRNAs were selectively increased (∼1.5–2.5-fold relatively to GAPDH mRNA). Here, the relatively high variability of target mRNA levels, both within (i.e., biological repeats) and among knock down experiments (using different ASOs), likely due to differences in transfection efficiency and ASOs' intrinsic activities, respectively, might be overcome by deleting the *SNORD83B* gene instead of knocking it down. As the levels of primary transcripts of these genes were unaltered, the authors concluded that SNORD83B silences targeted genes post-transcriptionally by a yet unidentified mechanism. Importantly, however, such studies will enable mechanistic studies of orphan snoRNA function.

With the advent of RNA-seq technology it became clear that many snoRNAs give rise to *stable* short RNA species (termed sdRNAs for snoRNA-derived RNAs) (49–53). Kishore *et al.* (41) have challenged the view that generation of sdRNAs is a common phenomenon based on sequencing snoRNA fragments cross-linked to *canonical* snoRNA protein partners. Yet, it is possible that even snoRNAs considered canonical, form additional RNPs. Common processing patterns were observed across snoRNAs (54), and the extent of processing is distinct for different snoRNAs in the same cell type (53,55,56), indeed suggesting that certain secondary structures and/or specific protein binding sites govern trimming patterns. At least some of the sdRNAs display microRNA (miRNA)-like features, such as dependence on Dicer processing (49), and association with argonaute (Ago) proteins (57), characteristic components of RNA-induced silencing complex (RISC). Most importantly, gene silencing activity for a number of miRNA-like sdRNAs was experimentally verified (50,57–59), whereas their precursors behaved as canonical snoRNAs in terms of being an integral part of snoRNPs. It should be stressed, however, that there is a threshold to the extent of Ago occupation required for detectable silencing activity; Thomson *et al.* (57) have noted that many sdRNAs (as well as short RNAs derived from precursors other than snoRNAs) bind Ago proteins, yet only highly bound snoRNA-derived miRNA-like species (irrespective of their expression levels; for example specific small RNA fragments derived from SNORA33 and SNORD56) were capable of producing measurable gene silencing effects in contrast to highly abundant but weakly bound small RNAs derived from tRNA, snRNA, vault, and Y-RNAs. It has been proposed that canonical miRNAs are evolutionary descendants of a subset of snoRNAs that have gained new functions (52). Thus, the involvement of distinct snoRNAs in post-transcriptional regulation of gene expression should not be an utter surprise.

Ono *et al.* (60) noted that SNORD88 family of snoRNAs harbors a segment of ∼20 nucleotides located downstream of the D′-box, displaying high level of complementary to endogenous pre-mRNA sequences, which they termed the M-box (Figure 4). SNORD88C was shown to be processed into shorter stable fragments (containing the M-box) in a cell type-specific manner, and proposed to regulate alternative splicing of *FGFR-3* (fibroblast growth factor receptor 3) transcript (55). Namely, ectopic expression of

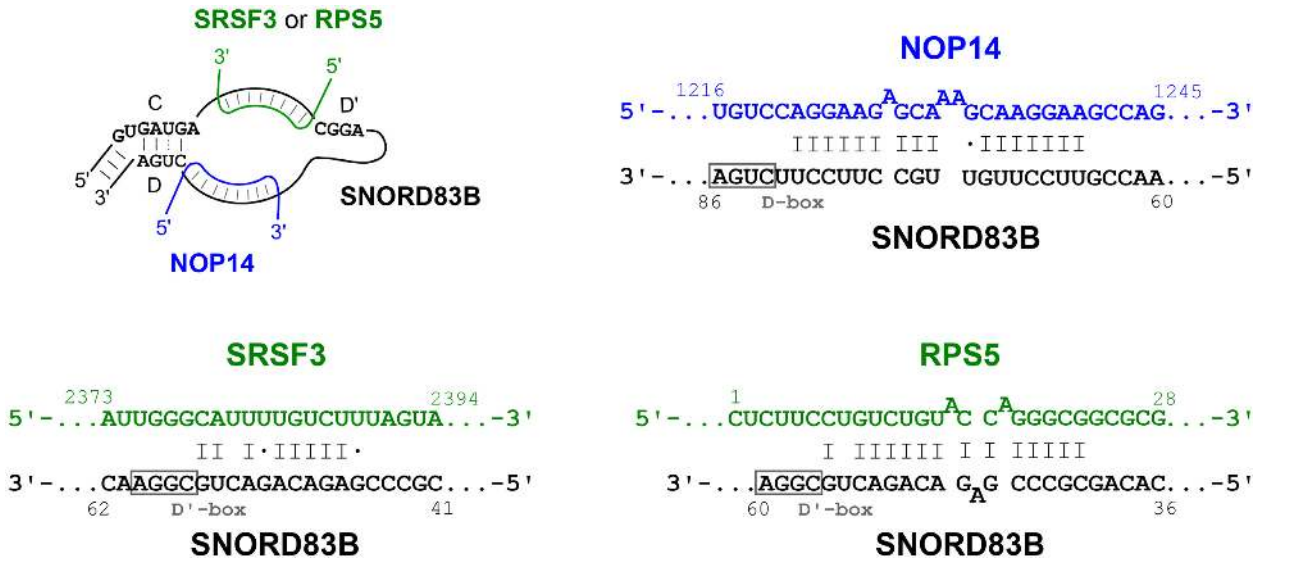

Figure 3. Predicted SNORD83B:mRNA interactions as inferred from unbiased mapping of RNA interactome by LIGR-seq (adapted from (48)). Protein subunits were omitted from snoRNP depiction for simplicity reasons. The biological significance of mRNA destabilization via snoRNA interactions remains to be determined. Note that base pairing occurs between mRNAs and the canonical antisense elements located immediately upstream of the D- or D'-boxes. SRSF3 – serine/arginine-rich splicing factor 3, RPS5 – small subunit ribosomal protein 5, NOP14 – nucleolar protein 14.

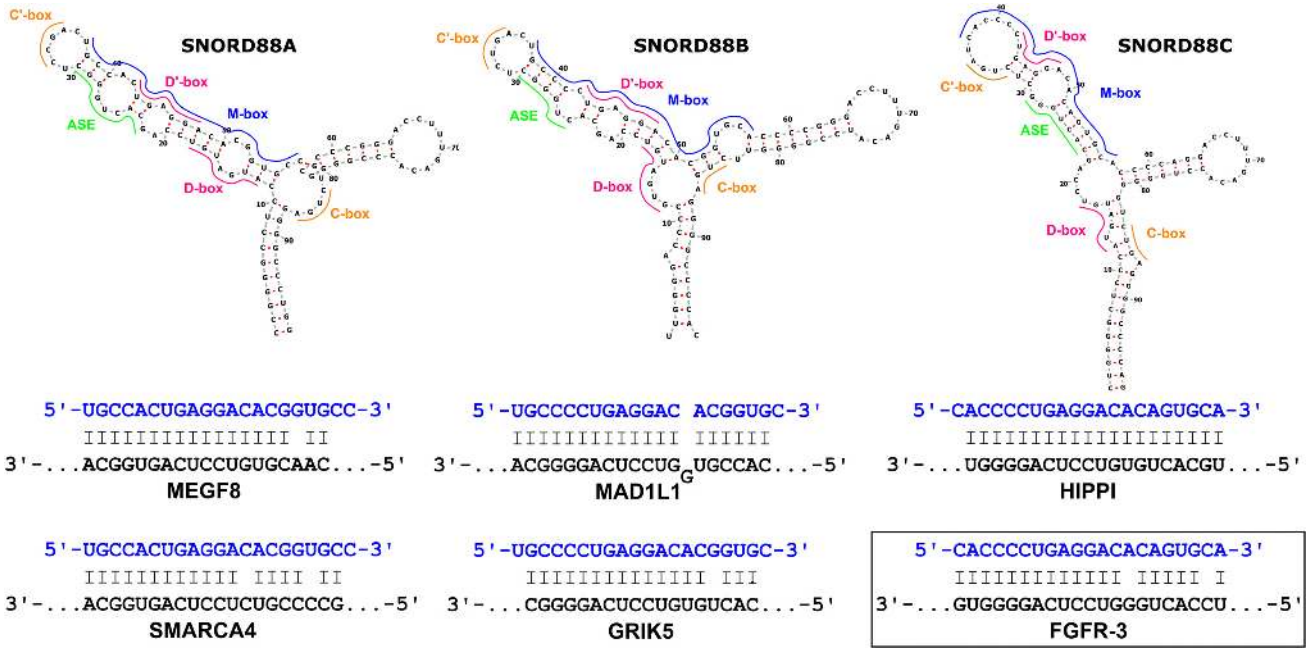

Figure 4. SNORD88A-C (upper panel; secondary structures predicted by RNAfold (62)) with characteristic elements of C/D-box snoRNAs highlighted: C/C'- and D/D'-boxes are shown in orange and pink, respectively, antisense elements (ASEs) complementary to 28S rRNA are depicted green. M-boxes are shown in blue. Lower panel displays sequence complementarities between the SNORD88A-C M-boxes and potential mRNA targets (adapted from (56,60)). The effect on *FGFR-3* pre-mRNA (boxed) processing was verified experimentally. MEGF8 – multiple epidermal growth factor-like domains protein 8, SMARCA4 – transcription activator BRG1, MAD1L1 – mitotic spindle assembly checkpoint protein, GRIK5 – ionotropic kainate glutamate receptor 5, HIPPI – intraflagellar transport protein 57 homolog, FGFR-3 – fibroblast growth factor receptor 3.

FGFR3 minigene harboring the presumed SNORD88C targeting region led to increased levels of a specific splice isoform (Δ8–10 FGFR3, encoding the soluble (decoy) receptor isoform (61)), likely due to sequestration of endogenous SNORD88C, whereas the splicing pattern did not change upon transfecting the cells with an empty vector or when a four nucleotide mutation was introduced to the *FGFR3* minigene region complementary to the SNORD88C guide element. In addition, overexpression of SNORD88C (but not the cognate D-box mutant) resulted in depletion of Δ8–10 FGFR3 splice isoform. However, knocking out endogenous SNORD88C (perhaps along with its paralogues that harbor highly homologous M-boxes and are encoded in separate introns of the same gene, *C19orf48*) or, better yet,

substituting them for SNORD88 variants with mutated M-boxes would provide means to rigorously interrogate the biological significance of M-boxes (if any), avoiding incomplete effects.

These observations inspired the design of so called snoMEN vectors (for snoRNA modulators of gene expression), a novel form of antisense technology in which the wild-type M-box of intronic SNORD88C (or SNORD47 (63)) is exchanged for artificial sequences directed to desired RNA targets. Efficient suppression of both, the co-transfected and endogenous protein-coding genes (60) as well as miRNA primary transcripts (64) was achieved with snoMEN, where knock-down efficiency was highly dependent on base pairing between the artificial snoRNA and target RNA (60). M-box-modified snoRNAs concentrated in the nucleolus, whereas RNA fragments corresponding to M-box region were present in the nucleoplasm but not in the cytoplasm (56). This is consistent with the fact that snoMEN can be targeted to introns and intron/exon junctions of pre-mRNAs, which are not amenable to siRNA-mediated knock-down (65). It is still not known what the exact silencing mechanism of snoMEN is, but knock-down activity showed dependence on fibrillarin (65) and C/D-box elements (60), indicating that proper snoRNA processing was essential for the observed effect. Interestingly, Ago2, the endonuclease component of RISC, is required for snoMEN gene silencing, but other factors, such as the up-frameshift-1 (UPF1), a protein believed to be essential for non-sense mediated decay (NMD), seem to be implicated in gene knock-down activity as well (65).

A recent study (preprint by Plewka *et al.*, doi: 10.1101/409250) showed that FUS (Fused in Sarcoma; a protein previously implicated in the regulation of genome maintenance, DNA repair, and RNA metabolism) negatively regulates the levels of mature snoRNA subgroup in HEK293T and HeLa cells. The authors speculate that FUS competes with canonical snoRNP proteins to induce snoRNA processing to sdRNAs. A group of sdRNAs derived from orphan SNORD68 was bioinformatically predicted to target KCNQ10T1-001 antisense transcripts encoded by the opposite strand of protein coding gene *KCNQ1* (voltage-gated potassium channel KCNQ 1), which might indicate a role for sdRNA68 in regulation of *KCNQ1* gene expression at the level of transcript stability. Indeed, a focused analysis confirmed downregulation of KCNQ1 mRNA and the cognate protein product in FUS knock-out cells (∼40% normalized to GAPDH mRNA and actin, respectively), while the opposite effect was observed in cells overexpressing FUS (ca. 50% and 20% upregulation for mRNA and protein levels, respectively). In both cases, the KCNQ10T1-001 antisense transcript levels displayed reciprocal regulation compared to the coding transcript, being 4-fold upregulated in FUS knock-out cells, and 2-fold downregulated in FUS overexpressing cells. Again, a SNORD68 knock-out cell line would allow for a more stringent verification of the proposed role for sdRNA68, as the capacity to regulate cellular KCNQ1 levels would be expected to be lost in such a model system.

SnoRNAs in regulation of alternative splicing

In search of non-canonical snoRNA functions, Falaleeva *et al.* (21) monitored the distribution of snoRNAs and their fragments in the nucleus of HeLa cells by RNA-seq. They found that approximately one quarter of C/D-box snoRNAs (as opposed to very few H/ACA-box snoRNAs) were present in a fraction that is devoid of fibrillarin, but enriched for spliceosomes and regulatory splicing factors. Surprisingly, among the identified SNORDs most were considered canonical with well-defined roles in rRNA methylation. In addition to canonical ASEs directed against rRNAs, however, the snoRNAs harbored an extensive segment of complementarity to bioinformatically predicted pre-mRNA targets, including introns and splice sites. These targeting sequences were unusual as they were fairly long, located outside the canonical antisense elements, and often contained C- and D-boxes. When several snoRNAs (SNORD2, -27, -60 and -78) were knocked-down, the splicing profile of their presumed pre-mRNA targets changed significantly. The direct interaction of SNORD27 and the alternative exon of transcription factor E2F7 pre-mRNA (Figure 5) was confirmed by RNA pull-down experiment and the fact that compensatory mutations in the targeted transcript rescued splicing modifying activity of cognate SNORD27 mutants. The authors speculated that this unusual group of snoRNAs associates with heterogeneous nuclear ribonucleoproteins (hnRNPs, well-established factors in splicing regulation (66)) and represses inclusion of alternative exons, perhaps by masking the cryptic splice sites. A similar mechanism might be exploited by SNORD88C in regulation of FGFR-3 transcript processing (55) (discussed above) and artificial SNORD24 analogues directed against HSPA-8 (heat shock 70 kDa protein 8) pre-mRNA developed by Stepanov *et al.* (67,68). Furthermore, the dependence of SNORD88C-derived snoMEN vectors' gene silencing activity on UPF1 (65) suggests that knock-down might be (at least in part) caused by frameshifts due to favoring alternative splice isoforms with early stop codons leading to nonsense mediated mRNA decay.

Brain-specific SNORD115 is perhaps the best characterized snoRNA implicated in splicing regulation. It harbors a conserved antisense element complementary to the alternative exon 5b of serotonin receptor 2c (Htr2c) pre-mRNA (26). A computational analysis of complementarity between the proposed targeted region on Htr2c pre-mRNA and the D-box-adjacent Snord115 guide region in 12 mammalian genomes revealed that perfect 18-nucleotide match is present only in primates and rodents (69). Although functional snoRNA ASEs may tolerate G:U base pairs and even mismatches to target RNAs, pairing of 2nd to 11th nucleotide of guide region typically adheres to canonical Watson–Crick rules and G:U pairing (70). Conversely, in many mammals (such as elephants and horses) there are mismatches within the D-box-proximal complementary Htr2c sequence, indicating that mRNA regulatory function of Snord115 might have first evolved through adaptive (compensatory) mutations in the Euarchontoglires clade, and may not be universally operative in all mammals.

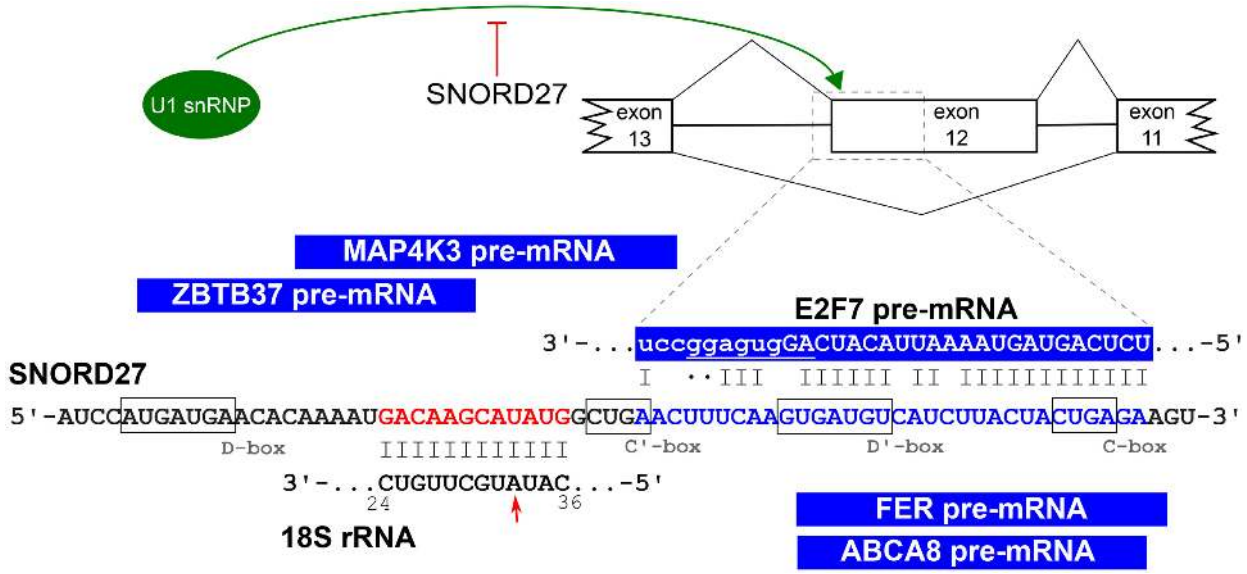

Figure 5. SNORD27 targets the E2F7 pre-mRNA alternative exon and the 5′ splice site, and presumably competes with U1 small nuclear ribonucleoprotein, thereby inducing exon skipping (adapted from (21)). Exons are shown as boxes and introns are indicated as thin lines (not to scale). Angled lines depict splicing patterns. Other predicted alternative splice sites within exon 12 are not shown for clarity. *In vitro* assays suggest that SNORD27 regulates splicing of multiple transcripts (interacting regions are shown as blue blocks aligned to the sequence of SNORD27). *E2F7* intron is depicted in lower case letters, while the alternative exon is presented in capital letters. 5′ splice site is underlined. In addition, SNORD27 guides 2′-*O*-ribose methylation on adenosine 33 of 18S rRNA (denoted by red arrow). MAP4K3 – mitogen-activated protein kinase kinase kinase kinase 3, ZBTB37 – zinc finger and BTB domain containing 37, FER – tyrosine-protein kinase Fer, ABCA8 – ATP-binding cassette sub-family A member 8.

The targeted Htr2c sequence is also subjected to enzymatic deamination of five closely spaced adenosines to inosines (termed A-to-I editing), leading to alteration of encoded genetic information and, in turn, amino acid sequence change within the second intracellular loop that contacts guanine nucleotide-binding proteins (71). Edited isoforms have diminished constitutive activity and potency compared to the unedited one (72,73). There are two receptor variants resulting from alternative splicing; inclusion of exon 5b leads to production of a long isoform capable of signal transduction, whereas exon 5b skipping results in a short isoform that is retained in the endoplasmic reticulum (ER) and sequesters the full-length receptor, preventing it to reach the plasma membrane (74). A-to-I editing of Htr2c pre-mRNA was shown to promote alternative exon 5b inclusion (75,76), enhancing production of full-length albeit less active receptor isoforms. Snord115 likely promotes production of full-length receptor isoforms with higher potency via two mechanisms: it blocks the silencer of splicing element (77), and at the same time it competes with adenosine deaminase enzymes responsible for Htr2c pre-mRNA A-to-I editing. Thus, it seems to promote alternative exon retention without the requirement for extensive A-to-I editing (78). The function of Snord115 in post-transcriptional regulation of Htr2c is consistent with the fact that Snord115 is expressed in neurons but absent in choroid plexus (brain structure mediating production of cerebrospinal fluid), where the full-length receptor isoform is not extensively produced (77). Of note, a recent study in mice constitutively expressing Snord115 in choroid plexus only identified A-to-I editing changes in Htr2c pre-mRNA (editing was slightly less abundant) but not alteration of splicing (79). Still, the association of Snord115 with alternative exon 5b was indirectly indicated by the observation of A-to-I edited Snord115 isoforms. Editing was selective for the Htr2c antisense element, suggesting local double-stranded RNA structure required for recognition by adenosine deaminases acting on RNA. Lack of observed effect on splicing in this *in vivo* model might be explained by absence of other factors missing in non-neuronal cells of choroid plexus. Currently, there are no mouse strains harboring *selective* deletion of *Snord115* gene cluster (Figure 6). Comparative analysis of potential A-to-I editing and splicing profile changes of Htr2c in wild-type and animals lacking Snord115 could be performed to clearly define the biological function of Snord115, and complementation experiments would allow for its validation.

Aside from Htr2c, Snord115 was shown to affect splicing patterns of several other genes in neuroblastoma cell line Neuro-2A (Table 1) (80). As these cells do not endogenously express Snord115, the biological importance of observed effect might be questionable; however, *in vivo* results from brains of Snord115 knock-out mice (TgPWS; see the *SnoRNAs implicated in Prader-Willi syndrome* section below) confirmed the dependency of alternative splicing for this transcript set on Snord115; Snord115 promoted alternative exon inclusion in Dpm2 and Pbrm1 pre-mRNAs, and induced alternative exon skipping in Ralgps1 and Taf1 pre-mRNAs, while for Crhr1 pre-mRNA opposite trends were detected *in vitro* and *in vivo* (attributed to likely difference in splicing regulators in Neuro-2A cells and mouse neurons). Ectopic murine Snord115 expression in human cell line HEK293 led to its processing to shorter fragments. The major processed sdRNA isoform contained C and D boxes but was devoid of the terminal stem sequence, and (in contrast to intact Snord115) did not associate with canonical snoRNP proteins, but rather hnRNPs (80), further sup-

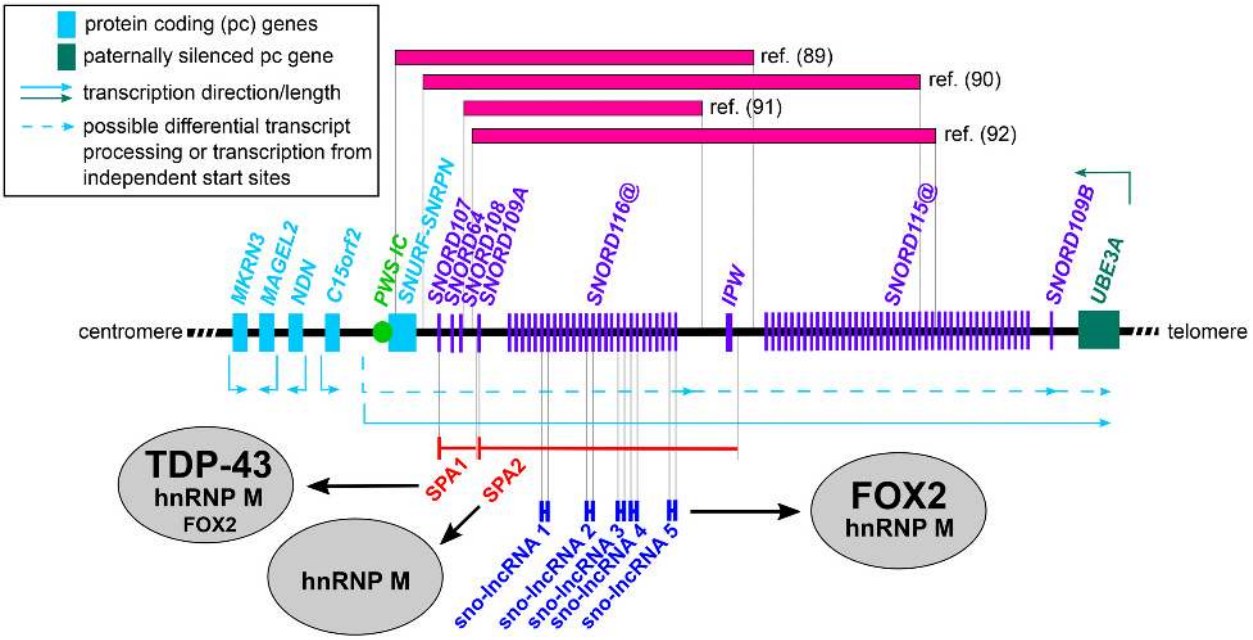

Figure 6. Genetic and expression map of the PWS critical region within the 15q11–13 locus (image not to scale; adapted from refs. (83,91,117)). The depicted genes are exclusively expressed from the paternal allele and are silenced on the maternal counterpart as a result of differential methylation of the bipartite PWS-imprinting center (PWS IC) located within the promoter and first exon of *SNURF-SNRPN*. A long non-protein-coding transcript (referred to as *SNURF-SNRNP-UBE3A AS*) initiating upstream of the PWS IC extends to overlap *UBE3A* in the antisense direction and silences *UBE3A* paternal allele by antisense-mediated mechanism. It also hosts intronic PWS snoRNAs SNORD107, SNORD64, SNORD108, SNORD109A, SNORD109B, as well as SNORD116 and SNORD115 gene clusters, containing 27 and 48 snoRNA copies, respectively. Documented microdeletions of the SNORD116 gene cluster leading to PWS phenotype are depicted above as pink boxes. sno-lncRNAs and SPAs are shown below as blue and red lines, respectively, with vertical bars depicting terminal snoRNA structures. The preference of PWS lncRNA for interacting with distinct RNA-binding proteins (gray circles) is portrayed by different font sizes.

porting the role of Snord115 in the regulation of splicing. Soeno *et al.* (24) used an antisense probe complementary to internal loop of Snord115 (intentionally avoiding the ASE) for affinity purification of Snord115-associated proteins from mouse brain cell nuclei. Using mass spectrometry (MS), they identified 17 proteins specific for the Snord115 snoRNP complex, previously implicated in pre-mRNA splicing and transcriptional regulation, such as hnRNPs and RNA helicases. Notably, the canonical snoRNP proteins could not be detected in the pull-down-enriched fraction by MS (although Snord115 was shown to co-immunoprecipitate with fibrillarin from the same nuclear extract).

Genes harboring intronic snoRNAs are generally very prone to alternative splicing that results in degradation of transcripts via NMD, and snoRNAs are often located in proximity of such alternative splice sites (81). This indicates that alternative splicing might serve to regulate snoRNA and snoRNP levels. A seminal study by Lykke-Andersen *et al.* (82) revealed that SNORD86, residing in an intron of the gene for snoRNP protein subunit NOP56, acts *in cis* as a master switch for modulating NOP56 cellular concentration. Remarkably, when cellular levels of NOP56 (and other snoRNP assembly factors, such as NOP58 and FBL) are high, SNORD86 in the context of NOP56 pre-mRNA takes on the 'snoRNP conformation', thereby deactivating the upstream splice donor and de-repressing the downstream splice donor, leading to retention of SNORD86-containing intron. The resulting NMD substrate mRNA (ns-mRNA) that contains a premature stop codon is exported to cytoplasm and cleaved by NMD endoribonuclease SMG6. The transcript is protected from degradation by the 5′ snoRNP structure (hence the name snoRD86 cytosolic snoRNA-capped and 3′ polyadenylated lncRNAs (snoRD86 cSPA)—in analogy to structurally similar nuclear SPAs (83) (see the *SnoRNAs implicated in Prader-Willi syndrome* section below)), and presumably acts as a long-lived decoy for snoRNP assembly factors, sequestering them away from nucleolus. In absence of snoRNP assembly factors, SNORD86 assumes the 'non-snoRNP conformation' in which D and D′ guide sequences pair with each other, forming a stable stem structure. In this setting, the upstream splice donor is active and the downstream counterpart is repressed, leading to excision of SNORD86-containing intron and production of both, NOP56-encoding mRNA and functional nucleolar SNORD86 snoRNP. The authors have elegantly shown that the described autoregulatory feedback loop is SNORD86-dependent, as neither minigene with SNORD86 deleted, replaced with its reversed complementary sequence nor exchanged for the unrelated SNORD71 did not succumb to modulation of alternative splicing by perturbation of snoRNP assembly factors. Thus, the structural switching mechanism seems to be governed by specific anatomical features of SNORD86. This snoRNA and its neighboring non-protein-coding region of *NOP56* gene are conserved within Eutheria clade, implying that the same mechanism governing cellular snoRNP levels operates in all mammals. NOP56

Table 1. SNORD115-targted pre-mRNAs (adapted from (80)). In the third column, introns and exons are depicted in lower case and capital letters, respectively

Gene name	Encoded protein	Complementarity	Targeted site	Function
Htr2c[*]	serotonin receptor 2c	pre-mRNA 5′-…CGUAAUCCUAUUGAGCAU…-3′ IIIIIIIIIIIIIIIII SNORD115 3′-…GCAUUAGGAUAACUCGUA…-5′	exon	full-length receptor formation
Dpm2	dolichol phosphate-mannose biosynthesis regulatory protein	C pre-mRNA 5′-…GUGAUUCU UUG guau…-3′ II•II•II III I•II CAUUAGGA AAC CGUA…-5′ SNORD115 3′-…G U U	exon/intron boundary	frameshift
Taf1	transcription initiation factor TFIID 250 kDa subunit	A G pre-mRNA 5′-…GU GUCCUGU UGAG AU…-3′ II •IIII•I IIII II CA UAGGAUA ACUC UA…-5′ SNORD115 3′-…G U G	exon	unknown domain
Ralgps1	Ras-specific guanine nucleotide-releasing factor RalGPS1	A pre-mRNA 5′-…UGU GUC GUUGAGUGU…-3′ •II •II •IIIII••I SNORD115 3′-…GCA UAG UAACUCGUA…-5′ U GA	exon	frameshift
Pbrm1	protein polybromo-1	au pre-mRNA 5′-…uaguccuguuga gca…-3′ II•IIII•IIII III AUUAGGAUAACU CGU SNORD115 3′-…GC A…-5′	intron	unknown domain
Crhr1	corticotropin-releasing factor receptor 1	A C pre-mRNA 5′-…CGUGG CCU AUUG GCA…-3′ III•• III IIII III SNORD115 3′-…GCAUU GGA UAAC CGU A U A…-5′	exon	deletion of hormone-binding domain

[*]not expressed in Neuro-2A cell line

expression needs to be tightly regulated as dysregulation can lead to defects in ribosome biogenesis, ultimately provoking nucleolar stress and activation of downstream cellular responses, such as apoptosis and cell cycle arrest due to p53 tumor suppressor activation (82).

SnoRNAs implicated in Prader-Willi syndrome

In humans, several orphan snoRNAs (including 48 and 27 copies of SNORD115 and SNORD116, respectively) are co-transcribed in introns of a large non-protein-coding transcript termed SNURF-SNRNP-UBE3A AS (Figure 6). Human SNORD116 are classified into three groups based on genomic location and sequence homology (group I: 116-1 to 116-9; group II: 116-10 to 116-24; and group III: 116-25 to 116-27) (84). Deletions in paternal chromosome 15q11-13 harboring these genes have long been associated with PWS, a complex multisystemic genetic disorder characterized by infant hypotonia and failure to thrive, followed by developmental delay, morbid obesity (if food intake is not strictly controlled), short stature, behavioral and cognitive problems (85). Although some of the behavioral, cognitive, and metabolic abnormalities may be explained by truncating mutations in the MAGEL2 protein coding gene present in the Prader-Willi critical region (86,87) (Figure 6) and dysregulation of the serotonergic system (presumably due to lack of SNORD115) (88), several case reports describing microdeletions which primarily encompass the SNORD116 cluster pinpoint this snoRNA as the principal genetic determinant of the condition (89–92). In addition, data from cell and rodent models support a major role for Snord116 in PWS. For example, there is evidence that loss of SNORD116 expression negatively affects neuronal differentiation of neuroblastoma cell line SH-SY5Y *in vitro* (93), while in mice with paternal Snord116 deletion endocrine pancreas developmental defects and neuroanatomical changes in brain (94), and cognitive defects (95) were documented. Mice represent an attractive model for study-

ing PWS due to highly conserved synteny between the human PWS critical region on chromosome 15q11-13 (Figure 6) and the orthologous locus on mouse chromosome 7C (differences include opposite orientation of the region with regards to centromeric/telomeric end of the chromosome, the presence of *Frat3* gene and the absence of *C15ORF2* and SNORD108, −109A, and −109B orthologues in mice, and the number of Snord116 and Snord115 tandem copies). Perhaps of importance, despite considerable sequence similarity between human and mouse SNORD116 (compared to poor *Snord116hg* evolutional conservation (96,97)), mouse Snord116 copies display lower sequence variability. They are fairly homologous to human SNORD116 from groups I and/or II, but are less similar to those belonging to group III (84). As mouse Snord116 deletion models fail to fully recapitulate the human PWS traits (98,99), it has been proposed that lack of group III-like Snord116 in mice might account for the non-overlapping phenotypes (84). A number of large paternal deletion (up to several Mb) or imprinting center deletion models, and single gene knock-out models were generated and thoroughly studied (reviewed in (98,100)). Here, we focus mainly on the *Snord116@* deletion models, as mounting evidence implicates this region in PWS pathophysiology. Nevertheless, lack of SNORD116 host gene (*SNORD116hg*) expression (rather than mature snoRNAs) might be the primary cause of PWS (101–103). To check this, *Snord116* transgenic mouse lines were generated on endogenous *Snord116@* knock-out background (see below), in which Snord116 was embedded in introns of different host genes (104). In these animals, the PWS-reminiscent phenotype could not be rescued, but this might also be attributed to very low expression levels of Snord116 compared to wild-type mice. Activation of silenced maternal *Snord116hg* in a mouse model harboring deletion of cognate gene on paternal chromosome, that resulted in Snord116 expression at ∼7.5-fold lower levels compared to wild-type littermates rescued the growth retardation, whereas the small phenotype persisted in *Snord116hg* knock-out animals expressing Snord116 at comparable degree from introns of a different host gene (105). Yet, the fact that Snord116 were not expressed in the same brain areas in the two mouse models precludes ruling out Snord116 as the non-protein-coding-RNA primarily responsible for the developmental condition.

Skryabin *et al.* (106) have deleted the *Snord116@* region via insertion of loxP sites at each side of the cluster in murine ESCs by homologous recombination and excision with ESC-electrophorated CRE recombinase. Genetically engineered ESCs were injected into blastocyst which was transferred to pseudopregnant recipients. Resulting male chimeras were bred with wild-type females to obtain heterozygous mice with paternal *Snord116@* deletion ($PWScr^{m+/p-}$). These mice were characterized by postnatal developmental retardation, reminiscent of human PWS subjects, but in contrast, did not become obese. Growth retardation persisted into adulthood. As the embryonal development was apparently not compromised, the authors concluded that postnatal developmental defects were likely secondary to poor feeding, mirrored by early failure to thrive phenotype in PWS infants. Ding *et al.* (104) constructed a similar murine *Snord116@* deletion model by a three-step approach. First, the *Snord116@* cluster in ESCs was flanked with loxP sites via homologous recombination, and the modified ESCs were used for generation of male chimeras. Heterozygous males were, in turn, mated with transgenic females carrying the CRE recombinase gene under the control of the ovary-specific Zp3 promoter. Finally, mating of doubly heterozygous (i.e. 2-loxP/+; Zp3-Cre/+) females with wild-type males led to CRE-mediated *Snord116@* cluster deletion *in vivo*. Snord116 knock-out mice ($Snord116^{lox/lox}$) again displayed normal embryonal development, but showed severely compromised postnatal growth, in line with findings of the earlier study. Mutant mice had a defect in motor learning and increased anxiety, both characteristic of PWS phenotype. Expression levels of insulin-like growth factor 1 were lower in mutant mice compared to their wild-type littermates, indicating that dysfunctional growth hormone (GH) pathway rather than poor feeding due to weak sucking reflex might be responsible for the developmental retardation. Similarly to PWS, no morphological abnormalities of the pituitary or its dysfunction were observed, suggesting that GH deficiency was likely secondary to hypothalamic dysfunction. When mice were kept on normal chow, there was no difference to the food intake between the $Snord116^{lox/lox}$ and wild-type subjects. On long term high-fat diet, however, Snord116 knock-out males (but not females) consumed less food, while mice of both genders gained less weight. The apparent resistance to high-fat diet-induced obesity and lower body fat content contrasts the human PWS phenotype. Yet, fasting-induced food intake at 6 and 10 months, in contrast to challenge at earlier age, disclosed hyperphagia in Snord116 knock-out mice, concomitant with higher ghrelin levels. Confirming suspicions that Snord116 deletion causes hypothalamic dysfunction, Qi *et al.* (107) have recently reported that in the same mouse model feeding related pathways in the hypothalamus are significantly altered as judged from gene expression analysis. Furthermore, selective deletion of *Snord116@* only from NPY-expressing neurons perfectly mimicked the global deletion phenotype. Here, increased levels of NPY (an orexigenic neuropeptide) mRNA were detected, likely responsible for the hyperphagic phenotype. This study proposed a central role of *Snord116@* in the control of NPY neuronal functions which might be dysregulated in PWS. In a following study (108), adeno-associated viral reintroduction of Snord116 in mid-hypothalamus of $Snord116@^{-/-}$ mice resulted in lower body weight gain due to higher energy expenditure; the effect was only seen at 6 (but not at 10) weeks of age and was specific to mid-region of hypothalamus. Hyperphagia was also induced by selectively disrupting *Snord116* expression in the mediobasal hypothalamus of *adult* mice via stereotactic injections of CRE recombinase-expressing adeno-associated virus in animals harboring floxed *Snord116@* cluster (109). Another paper (110) described the effects of global *Snord116@* deletion when conferred in adult mice, again avoiding developmental influences of *Snord116@* deficiency. In contrast to the global germline and hypothalamus-specific *Snord116@* deletion model, adult-onset global *Snord116@* knock-out resulted in normal growth, reduced food intake and increased adiposity without changes in body weight. Such differences in mouse PWS models show the complexity of

Snord116@-governed mechanisms, and suggest that developmental and/or tissue factors modulate this RNA's function. In line with this, Zhang *et al.* (111) have reported that Snord116 expression in mice is regulated developmentally (being highest in hypothalamic nuclei at weaning and young adult stages, whereas Snord116 were expressed at lower levels and more uniformly in the embryonic brain).

With regards to the proposed function of SNORD115 in regulating the serotonergic activity in the central nervous system (see the *SnoRNAs in regulation of alternative splicing* section above), mouse models corroborate *in vitro* findings. For example, mice with paternal PWS imprinting center deletion (PWS-IC$^{+/-}$; hence lacking Snord115 expression along with all other PWS critical region genes) showed changes in specific Htr2c-related behaviours (112), in line with increased A-to-I editing believed to be a direct consequence of Snord115 loss. Moreover, PWS-IC$^{+/-}$ mice were reported to display tolerance to preferential Htr2c agonist WAY-161503 (113), and the blunted anorexic effect was attributed to increased proportion of Htr2c short splice isoform in hypothalamic pro-opiomelanocortin neurons. Furthermore, perturbation of alternative splicing for Snord115-targeted transcripts shown in murine neuroblastoma cell line (80) was also observed in TgPWS mouse model, harbouring a 5-Mb deletion including the entire PWS-homologous region (114).

The PWS behavioral phenotype somewhat overlaps with that observed in subjects with autism spectrum disorder (ASD) (115). A recent genome-wide study (116) of human post mortem brain samples from ASD and 15q duplication cases implicated orphan snoRNAs of the imprinted 15q11 and 14q32 loci in autism pathogenesis. The predicted snoRNA targets showed changes in splicing and were enriched in genes displaying allele-specific expression (i.e. preferential expression of one allele over the other) and those carrying *de novo* ASD-associated risk mutations. Notably, the asymmetric allele expression in ASD was biased towards the minor alleles. The authors suggest that snoRNA-mediated splicing alterations of dosage-sensitive genes (harboring *de novo* risk variations) might explain the proneness to ASD.

The Chen lab published a series of papers revealing yet another intriguing mechanism of splicing regulation by snoRNAs, specifically by SNORD116. Analyzing RNA-seq data of poly(A)- and rRNA-depleted RNA fraction of 200 nt and above from human embryonic stem cells (ESC), they identified a new class of long non-protein-coding RNAs whose ends corresponded to SNORD116 paralogues (termed snoRNA-ended long non-coding RNAs or sno-lncRNAs for short; Figure 6) (117). As the C- and D-boxes of terminal SNORD116 copies were essential for pre-RNA processing and stability, and sno-lncRNAs co-immunoprecipitated with canonical snoRNP proteins, the authors concluded that terminal snoRNP assembly serves to prevent exonucleolytic degradation of the transcript. The sno-lncRNAs were retained in the nucleus, accumulating near the sites of processing, but not nucleolus or CBs, and were (in contrast to many other lncRNAs) not associated tightly with chromatin. Instead, they exerted their function by sequestering the splicing factor FOX2 to subtly alter splicing patterns in cells as deduced from CLIP-seq experiments and RNA-seq data upon PWS sno-lncRNA knock-down. Validating this mechanism of action was the notion that many alternative exons were oppositely affected by FOX2 knockdown and PWS sno-lncRNA depletion. FOX2-titration supposedly restricts the effect on splicing modulation to specific subnuclear zones rather than directing splicing patterns universally throughout the nucleus. A further study (83) identified two Prader-Willi locus lncRNAs requiring 5′ snoRNP cap to protect them from exonucleolytic degradation. The 5′ snoRNA-capped and 3′ polyadenylated lncRNAs (SPAs; Figure 6) were highly abundant in ESCs and normal induced pluripotent stem cells (iPSCs; but not those derived from PWS subjects), and, similarly to sno-lncRNAs, concentrated at or near their processing site on the paternal chromosome. SPAs interacted with well-known RNA-binding proteins TDP-43, FOX2 and hnRNP M, involved in several aspects or RNA metabolism, including splicing regulation. SPA knock-out in human ESCs led to changes in splicing patterns for 348 genes; some of the changes were also confirmed in PWS iPSCs. The sno-lncRNAs and SPAs are not phylogenetically conserved, being observed in human but absent in mouse (83,118). It might be worthwhile to check whether ectopically expressed human sno-lncRNAs and SPAs locally deplete splicing factors in brain tissue of *Snord116@* knock-out mice, and analyze potential changes in global splicing profiles. Furthermore, since their functional units do not rely on SNORD116 sequence itself, it would be informative to examine potential splicing factor sequestration by the ectopically expressed non-protein-coding *SNORD116hg* transcript lacking introns in *Snord116@* knock-out animals, thus checking whether the proposed biological role of sno-lncRNAs and SPAs can in fact be attributed to the SNORD116 host gene.

SnoRNAs as regulators of cholesterol homeostasis

Cellular cholesterol levels are maintained at a steady level by endogenous synthesis and uptake, which are regulated by negative feedback loops (119). When cholesterol levels decrease, transcription factors termed sterol regulatory element-binding proteins (SREBPs) are activated to promote transcription of genes required for *de novo* cholesterol synthesis and low density lipoprotein (LDL) internalization. When cholesterol levels increase, SREBPs are repressed, while some of the extra cholesterol is trafficked to mitochondria, where it is oxidized to side-chain oxysterols. These, in turn, activate liver X receptors, nuclear receptors that promote transcription of genes responsible for export of excess cholesterol from the cell. As cholesterol levels decline, there is a reduction of oxysterol synthesis, effectively repressing further cholesterol efflux. Receptor-mediated LDL endocytosis is a major source of exogenous cholesterol, and cholesterol is distributed to plasma membrane as well as multiple organelles via endolysosomes. When levels of cellular cholesterol are high, it is trafficked from plasma membrane to ER independently from the endolysosomal route. In ER, cholesterol inhibits SREBP processing and activation and promotes re-esterification of cholesterol by the acyl coenzyme A (CoA):cholesterol acyltransferase. Delivery of plasma membrane cholesterol to

mitochondria allows for local enzymatic production of 27-hydroxycholesterol, which indirectly represses SREBP processing in ER.

Evidence of an unexpected role for specific snoRNAs in mediating intracellular cholesterol trafficking came from 2 forward genetic screen studies (120,121). In both cases researchers used retroviral promoter trap mutagenesis to randomly disrupt genes in CHO cells, hijacking endogenous upstream promoters for expression of selection marker bestowing resistance to neomycin. Cells that survived a round of neomycin treatment were subsequently subjected to cholesterol starvation, followed by treatment with amphotericin B (a polyene antibiotic that lyses cells by forming pores in cholesterol-rich membranes) and LDL to select for clones deficient in trafficking of newly plasma membrane-incorporated exogenous cholesterol to ER. The first study (120) recovered a mutant cell line displaying an increased rate of *de novo* cholesterol synthesis, while esterification of plasma membrane-derived cholesterol was decreased, probably as a result of cellular cholesterol level sensing defects. Surprisingly, the underlying insertional mutation was present in the non-protein-coding Snord60 host gene (*U60snhg*). Complementation of the *U60snhg*-haploinsufficent cell line with the murine orthologue rescued the cholesterol trafficking defect, and the phenotype was only restored when the cells were transfected with wild-type *U60snhg* but not analogues with mutated D′-box and ASE. Thus, Snord60 likely interacts with RNAs other than or in addition to its presumed canonical target (28S rRNA). No studies addressing the Snord60 mechanism of action have been conducted. Snord60 expression/stability seems to correlate with intracellular cholesterol levels both in wild-type and mutant CHO cells, indicating possible reciprocal regulation. Interestingly, a chromatin immunoprecipitation (ChIP)-seq study (122) previously found that *U60snhg* promoter in HepG2 cells is occupied by transcription factor SREBP1, the master switch of cholesterol uptake and synthesis, suggesting a direct link between cellular cholesterol regulating machinery and SNORD60 expression at transcriptional level. More recently, a similar phenotype was attributed to haploinsufficiency for snoRNAs Snora73A and Snora73B, 18S rRNA-processing chaperones harbored in consecutive introns of the non-protein-coding gene *Snhg3* (121). Transcriptomes of NIH 3T3 mouse fibroblasts in which Snora73 was either overexpressed (OE) or stably knocked down (KD) were compared by using microarray analysis to identify differentially expressed mRNAs, potentially representing Snora73 downstream targets. One of the few genes that were upregulated in KD (>4-fold (GAPDH-normalized) and ∼2-fold (HSP90-normalized) at mRNA and protein levels, respectively) and downregulated in OE cells (approx. 90% for both mRNA and protein), the hypoxia-upregulated mitochondrial movement regulator (*Hummr*), a mitochondrial adaptor protein implicated in mitochondrial motility, contained a region of complementary to the highly conserved but unusual Snora73 antisense element (termed m1/m2) of the 3′ internal loop (Figure 7A); direct interaction of Snora73 and Hummr mRNA was later confirmed by pull-down assay. Finally, *Hummr* overexpression resulted in a phenotype identical to Snora73 KD, leading to decrease in cholesterol esterification, while *Hummr* knockdown phenocopied *Hummr* downregulation by Snora73 OE, increasing cholesterol esterification. Notably, Snora73 and *Hummr* display opposite expression profiles in mouse ovaries, and are developmentally regulated to control mitochondrial steroid hormone synthesis. These observations are consistent with the model in which Hummr mitigates esterification of plasma membrane-derived cholesterol in ER by diverting cholesterol to mitochondria via enhancing ER-mitochondrial contacts (complexes termed MAM (for mitochondrial associated ER membranes), well-known sites of lipid exchange between ER and mitochondria) (Figure 7B).

SnoRNAs as regulators of metabolic and oxidative stress

At the outer mitochondrial membrane, free fatty acids are converted to acyl carnitines by the action of carnitine acyltransferase I, and subsequently translocated to the matrix, where they undergo β-oxidation. The released acetyl-CoA enters the Krebs cycle, and is gradually oxidized; the resulting reducing equivalents are transferred to electron transport chain for ATP synthesis. Extensive β-oxidation attenuates further mitochondrial free fatty acid uptake via formation of malonyl CoA, an inhibitor of carnitine acyltransferase I. However, excess free fatty acids (as well as glucose) can cause formation of reactive oxygen species (ROS), leading to mitochondrial dysfunction, ER stress with Ca^{2+} release, and cell death in a process known as lipo(gluco)toxicity. The disruption of Ca^{2+} regulation by chronic oxidative stress is believed to contribute to type II diabetes development (123).

Michel *et al.* (124) resorted to retroviral promoter trap mutagenesis coupled with palmitate treatment of transduced CHO cells to identify loss-of-function mutations for resistance to oxidative stress. The causative mutation was present in the gene *Rpl13a* encoding the 60S subunit ribosomal protein L13a. Unexpectedly, it was the haploinsufficiency for three out of four intronic C/D-box snoRNAs (Snord32A, -33 and -35A) rather than the protein coding portion of the gene that was responsible for the observed phenotype. Palmitate exposure brought ∼5–6-fold upregulation of the *Rpl13a* snoRNAs but not the mature mRNA, whereas concomitant knockdown of Snord32A, -33 and -35A in murine myoblasts phenocopied palmitate resistance of the *Rpl13a*-deficient CHO mutant. Moreover, the researchers confirmed their findings *in vivo*, demonstrating that *Rpl13a* snoRNAs are required for propagation of oxidative stress in lipopolysaccharide (LPS)-challenged mice. Under lipotoxic conditions, the *Rpl13a* snoRNAs accumulated in the cytoplasm of murine myoblasts (whereas their nuclear levels were unchanged), suggesting potential non-canonical snoRNA function in the regulation of translation. In a further study (125), the same research group created a mouse model homozygous for deletion of *Rpl13a* snoRNAs from the hosting introns. Fibroblasts isolated from '*Rpl13a*-snoless' mouse embryos had diminished ability to amplify ROS and were resistant to ROS stimulation by exogenous hydrogen peroxide. The *Rpl13a*-snoless mice reacted to glucose challenge by enhanced insulin secretion, which was attributed to altered mitochondrial metabolism

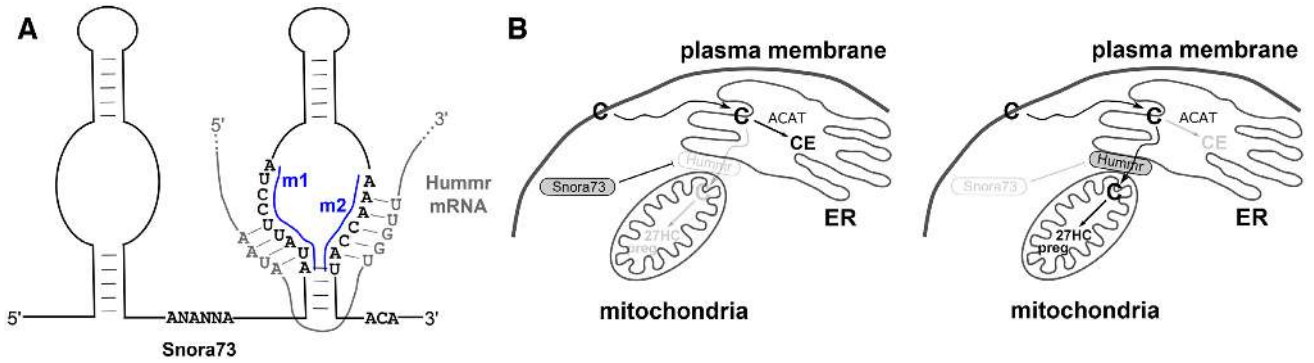

Figure 7. Snora73 targets Hummr mRNA to regulate cellular cholesterol trafficking (adapted from (121)). (**A**) Proposed interaction between Snora73 and Hummr mRNA. Conserved sequence motifs m1 and m2 within the internal loop of 3′ hairpin of Snora73 are shown in blue. Note that the antisense element is located at the lower part of the loop in contrast to canonical H/ACA-box snoRNAs (compare with Figure 1C). Protein subunits were omitted from snoRNP depiction for simplicity reasons. (**B**) Model of Snora73-Hummr cholesterol trafficking pathway. When Snora73 levels are high (left), Hummr expression is silenced. Thus, cholesterol (C) is retained in the endoplasmic reticulum (ER) where it is esterified (CE) by acyl CoA:cholesterol acyltransferase (ACAT), and only basal levels reach mitochondria. Conversely, when Snora73 is deficient (right), Hummr silencing is alleviated. Hummr is essential for formation of ER-mitochondrial contacts, indirectly enabling cholesterol flux to mitochondria (diverting it from the ACAT-accessible pool in the ER), where it is converted to 27-hydroxycholesterol (27HC) and steroid hormones (preg stands for pregnenolone, a common steroid hormone precursor).

(126). When the *Rpl13a*-snoless mice were crossed with diabetogenic counterparts of three different genetic backgrounds, the *Rpl13a* snoRNA loss-of-function mutation protected animals against hyperglycemic stimuli that otherwise cause damage to pancreatic β cells, providing very strong evidence for the non-canonical function attributed to *Rpl13a* snoRNAs. Transcriptome comparison of *Rpl13a*-snoless and wild-type islets only revealed 6 differentially expressed genes, none of which was previously associated with response to ROS, nor did they display any sequence complementarity to Snord32A, -33, -34 and -35A, making them unlikely direct targets of *Rpl13a* snoRNAs. Recently, Elliott *et al.* (127) have shown that SNORD32A (and SNORD51 that harbors highly similar D'-box ASE) target peroxidasin (PXDN) mRNA for 2′-*O*-ribose methylation by fibrillarin at adenosine residue A3150 within the coding region (Figure 8A). The modification led to increased mRNA stability (i.e. PXDN mRNA levels increased), but significantly inhibited translation efficiency due to steric blockade of interactions between rRNA and the phosphoribose backbone of the mRNA-tRNA minihelix. Peroxidasin is a peroxidase consuming hydrogen peroxide to catalyze extracellular production of highly reactive hypobromous acid (128), and thus represents an attractive candidate to explain the mechanism behind *Rpl13a* snoRNAs-induced oxidative stress (Figure 8B). SNORD32A, and the presumed PXDN mRNA target sequences are conserved in fly, mouse, and human (127). It is tempting to speculate that similar epitranscriptomic modifications exerted by snoRNAs might constitute a more widespread post-transcriptional gene regulating network.

Interestingly, Zhang *et al.* (118) found evidence of species-specific expression of sno-lncRNA flanked by Snord33 and Snord34; due to differences in alternative splicing, the sno-lncRNA was highly expressed in mouse ESCs, but only slightly in rhesus ESCs and absent in human cell lines. The relevance of this sno-lncRNA is unclear; however, the alternative processing of Rpl13a pre-mRNA, producing a splice isoform with an open reading frame shift at the Rpl13a protein C-terminus in addition to full-length protein, might indicate a role for alternative splicing in the regulation of 60S ribosome subunit function in a species-specific manner. Rpl13a has previously been shown to participate in translational modulation of specific mRNAs as a component of interferon-γ-activated inhibitor of translation (GAIT) complex (129,130). Whether the change of intronic neighborhoods due to snoRNA deletion affects *Rpl13a* splicing patterns has not been investigated.

Proper splicing mechanisms are also essential for release of intronic snoRNA as exemplified by the fact that loss-of-function mutation in one of the alleles encoding SmD3, a small nuclear ribonucleoprotein component of spliceosomes, protects CHO cells against lipotoxicity (131). The *Snrpd3* haploinsufficiency caused impaired basal expression and lipotoxic cytosolic accumulation of a subset of H/ACA- and C/D-box snoRNAs, including *Rpl13a* snoRNAs, explaining the ROS-resistant phenotype.

Doxorubicin-induced oxidative stress was reported to cause indiscriminate C/D-box snoRNA shuttling from nucleus to cytosol (132). Cytosolic accumulation was also detected for H/ACA-box snoRNAs and scaRNAs, albeit to lesser levels. Focusing on *Rpl13a* snoRNAs, Rimer *et al.* (133) reported that LPS stimulation induced snoRNA secretion by extracellular vesicles from cultured murine macrophages, and that levels of Snord32/-33A/-34/-35A increased in plasma of LPS-treated mice (∼2-6-fold relative to spike-in control) and human volunteers (∼2-fold), raising the question of whether snoRNAs can function in distant tissues. In addition to their proven non-canonical function, *Rpl13a* snoRNAs guide 18S and 28S rRNA 2′-*O*-ribose methylation, as demonstrated by comparing methylation levels of predicted targeted sites in macrophages isolated from wild-type and *Rpl13a*-snoless mice (133). Although a previous study did not detect perturbations in the extent of rRNA methylation at *Rlp13a* snoRNA-targeted sites upon lipotoxic/oxidative stress (124), this might well be due to insignificant snoRNA nuclear level change. To test

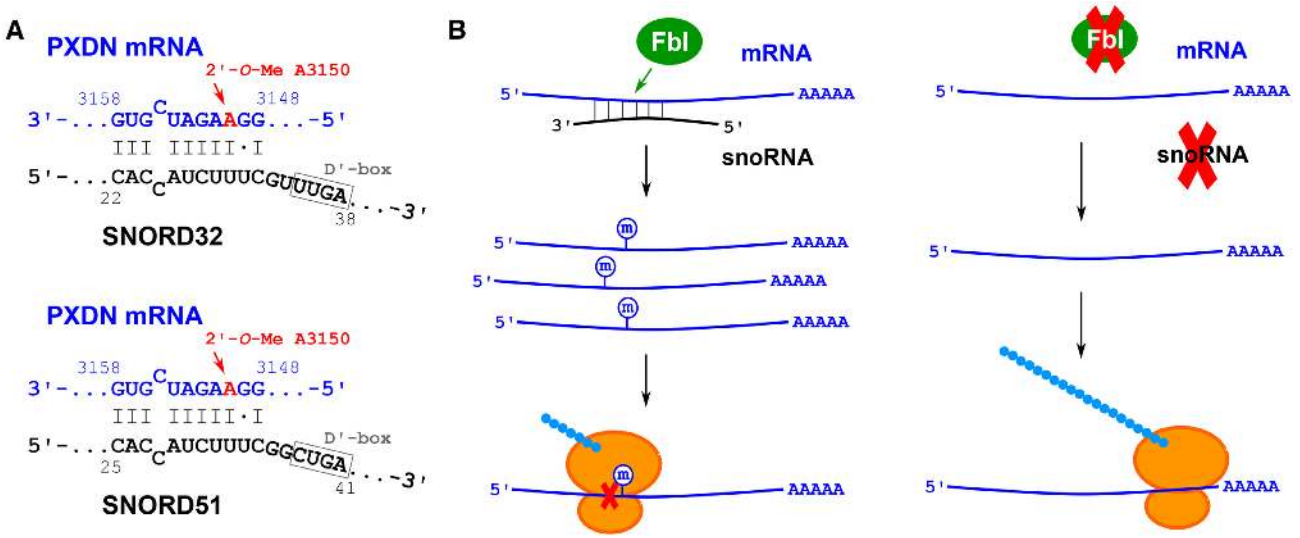

Figure 8. SNORD32 and -51 regulate the expression levels of peroxidasin (PXDN) post-transcriptionally (adapted from (127)). (**A**) Predicted interactions between the human SNORD32/-51 and PXDN mRNA. The nucleotide targeted for 2′-O-ribose methylation is shown in red. (**B**) Proposed model of PXDN mRNA translational regulation. SNORD32/-51 target PXDN mRNA for 2′-*O*-ribose methylation by fibrillarin, resulting in increase in mRNA abundance but decreased protein expression (left). In absence of SNORD32/-51 (or fibrillarin), the PXDN mRNA is not subject to 2′-*O*-ribose methylation, leading to decreased mRNA stability and alleviated translational suppression (right). Fbl – fibrillarin.

the potential long-range functioning of extracellular snoRNAs, the authors used a very sensitive parabiosis model in which wild-type mice were surgically joined to *Rpl13a* snoRNA knock-out mice, sharing the blood circulatory system. They found evidence of increased rRNA methylation 3 weeks after surgery in enterocytes (rapidly proliferating cells with intense rRNA biogenesis) in knock-out parabionts in comparison to knock-out controls, while in hepatocytes (that divide much slower) no change was apparent. The authors were unable to detect *Rpl13a* snoRNAs in knock-out parabiont tissues by qPCR, indicating that long-range distribution of snoRNAs is not very extensive and/or that snoRNAs are relatively short-lived in the recipient tissues in contrast to rRNA modifications they leave behind. Nevertheless, this complex experiment demonstrated that *Rpl13a* snoRNAs perform dual functions (i.e. guide rRNA methylation along with serving as oxidative stress promoters), and can exert their effect (at least the canonical one) over long distances.

Role of snoRNAs in memory consolidation and learning

In situ hybridization analysis (134) revealed that several orphan snoRNAs (Snord115, Snord116, Snora35 and the rodent-specific C/D-box snoRNA MBII-48 (also termed AF357425)) display uneven expression levels across mouse brain structures, being especially abundant in the ventral hippocampus (except for Snord116, which is equally strongly expressed also in dorsal hippocampus, amygdala and cerebral cortex). As hippocampus oversees fundamental learning and memory processes (including explicit/declarative memory), Rogelj *et al.* (134) hypothesized that this group of brain-specific snoRNAs might play a role in higher brain functions. They designed an experiment involving contextual fear conditioning (a Pavlovian learning method that establishes association between stimuli (e.g. sound) and their aversive consequences (e.g. electric shock)) and monitored hippocampal expression changes of the four snoRNAs during memory consolidation. Indeed, two snoRNAs, Snord115 and MBII-48, displayed short-term up- (∼40%) and downregulation (∼25%), respectively. The expression changes were specific for contextual conditioning, as neither new environment nor audio or shock stimuli by themselves had any significant effect on snoRNA levels. These observations suggest a potential role of Snord115 and MBII-48 in memory consolidation. To support functional analyses of snoRNAs, it would be worthwhile to examine transcriptome shifts during simple learning tasks, taking advantage of single-cell RNA-seq approaches (considering the structural and functional complexity of hippocampus (135)).

In contrast to SPAs and sno-lncRNAs (see the *SnoRNAs implicated in Prader-Willi syndrome* section above), the recently characterized nucleolar long non-protein-coding RNA LoNA (also called GM17382 (136)) harbors two C/D-box snoRNA elements which are not required for proper RNA processing or stability of its precursor, but rather have functional roles in sequestering fibrillarin, reminiscent of snoRD86 cSPA reported by Lykke-Andersen ((82); see the *SnoRNAs in regulation of alternative splicing* section above). LoNA is highly expressed in Neuro-2A neuroblastoma cells and mouse hippocampus, but its levels rapidly drop upon neuronal stimulation *in vitro* and in brains of mice subjected to behavioral tests (such as Morris water maze and object-context discrimination training). LoNA thus seems to serve as a sensor of neuronal activity, and its cellular concentration inversely correlates with levels of pre-rRNA as well as mature rRNAs. LoNA contains a 5′ nucleolin-binding motif to sequester nucleolin activity, thereby negatively affecting the process of rDNA transcription via modulation of the chromatin's epigenetic state. In addition, LoNA's 3′ C/D-box elements compete with

canonical snoRNAs for fibrillarin binding, leading to perturbed methylation status of rRNAs. The reduced rRNA production results in diminished ribosome levels and, in turn, attenuation of protein synthesis. Because the translational efficiency for several synaptic proteins (such as AMPA receptor GluR2, NMDA receptors NR1/2A/2B, and synaptophysin) is impaired, LoNA indirectly modulates synaptic plasticity as confirmed in mouse models. Specifically, LoNA knock-down mice outperformed control animals in behavioral tests, while mice that underwent LoNA administration to hippocampus displayed impaired spatial learning and memory. Remarkably, LoNA-deficient APP/PS1 transgenic mice (an Alzheimer model harboring human amyloid precursor protein and presenilin 1 mutated genes, and characterized by amyloid deposition, impaired learning, increased LoNA abundance and reduced brain rRNA levels) showed rescue of learning and memory defects. Ultimately, animal models harboring deletions of LoNA nucleolin- and/or fibrillarin-binding motifs or the entire *LoNA* gene will serve to validate this lncRNA's proposed biological role. Li *et al*. (136) report on identification of a long non-protein-coding RNA in human (termed RP11-517C16.2) which harbors the nucleolin-binding motif and C/D-box elements, suggesting that similar rRNA modulation mechanisms affecting learning and memory processes might operate in human as well.

METHODS OF SNORNA FUNCTIONAL ANALYSIS

SnoRNAs appear to be very heterogeneous with regards to structure, target RNA recognition, choice of partner proteins, and the mechanism of action. Functional analysis of snoRNAs thus requires an interdisciplinary approach, traditionally combining expression profiling, and *in silico* target prediction followed by wet lab validation (e.g., directly by demonstrating the association between snoRNA and its presumed target, or indirectly through determining target RNA's chemical modifications or abundance upon snoRNA knock-down/overexpression). Recent methods of unbiased RNA interactome profiling have proven invaluable for snoRNA target identification, and RNA-protein interrogation techniques have enabled insight into (alternative) snoRNP assembly. New sophisticated approaches are being developed for high-throughput transcriptome-wide RNA modification analyses, indirectly revealing and validating canonical snoRNA targeted sites. In addition, genetic screening campaigns have disclosed some unexpected roles for snoRNAs. In this final section, we briefly review the current snoRNA profiling toolbox.

SnoRNA expression profiling

Having an intermediate size (60–300 nt), snoRNAs are long enough to be accurately quantified by conventional qPCR after being reverse transcribed (RT) by random priming (e.g. (78,137)). Alternatively, target-specific stem loop primers introducing a universal 5′ cDNA sequence have been used for RT (133), allowing specific detection of mature snoRNAs but not snoRNA sequences on genomic DNA or pre-mRNA templates. Another option is to polyadenylate (sno)RNAs *in vitro* and perform RT with an oligo(dT) primer carrying a 5′ universal adapter (138). RNA-seq has transformed the field of (sno)RNA biology, enabling unprecedented expression profiling (e.g., modest changes in expression levels can be addressed owing to extremely high sensitivity) as well as a detailed look into intricate RNA processing (4,55,83,117). A common approach for RNA-seq library construction is based on ligation of universal adaptors to RNA molecules for RT and cDNA amplification. One should consider, however, that RNA quantification (including snoRNAs) can be severely affected by differences in adapter ligation efficiencies, as well as complex RNA structures, post-transcriptional modifications, and differences in G/C-content, that are all potential sources of bias (139). Conventional methods, such as the semi-quantitative northern blotting and RNase protection assay (RPA) are therefore still used extensively for validation purposes. In RPA, an *in vitro*-transcribed uniformly ^{32}P-labeled single-stranded antisense probe is hybridized to target RNA, protecting it from subsequent degradation by single strand-cleaving RNases A and/or T1. Finally, high resolution electrophoresis is performed, followed by sensitive autoradiography to reveal the presence, size, and relative levels of probe-protected RNA. For example, RPA has been used for confirming snoRNA processing patterns of Snord115 first detected by cloning and sequencing of fragments (80).

Bioinformatic target prediction

A number of bioinformatic tools, such as snoTARGET (140), RNAsnoop (141) and PLEXY (142), have been developed for identifying RNA targets of snoRNAs. However, these large input sequence-scanning programs are typically based on the assumption that snoRNAs adhere to canonical folding patterns, and snoRNA:target RNA interactions are scanned considering constraints observed for validated snoRNA:rRNA pairs, which might not be the case for all members of the family. Furthermore, C/D-box snoRNAs harbor relatively short antisense elements that tolerate a number of mismatches (70), while antisense elements of H/ACA-box snoRNAs are bipartite in addition to being short, making target identification relatively unreliable. Indeed, Kishore *et al.* (80) had to test over a hundred computationally predicted phylogenetically conserved targets of Snord115 experimentally to identify 5 transcripts (Table 1) whose splicing showed dependence on this snoRNA. In addition, in some C/D-box snoRNAs, segments other than the canonical ASE 5′ to D/D'-box were observed to enhance cognate snoRNP's methylation activity (143).

Exogenous modulation of snoRNA levels

Blocking the activity of an endogenous snoRNA is a useful approach of screening for its functions (e.g. coupled with phenotypical or comparative transcriptome analyses) or verifying its presumed targets. As snoRNAs are primarily nuclear residents, RNA interference (a well-established experimental gene silencing technology), is ineffective for snoRNA knock-down. Instead, synthetic chimeric antisense oligonucleotides (ASOs) enable efficient and selective snoRNA depletion both *in vitro* and *in vivo* (144,145).

These ASOs are typically 20 nt long, contain phosphorothioate linkages, and are comprised of 10 central deoxynucleotides with 5 terminal 2′-*O*-methoxyribonucleotides at each side; the modifications protect them from degradation by exonucleases. Upon base paring with target nuclear (sno)RNA, the heteroduplex is recognized by RNase H, cleaving the RNA. ASOs are delivered to cells by nucleofection. Conversely, snoRNAs can be ectopically expressed in host cells, and often vectors encoding snoRNAs in their native intronic environment are used to ensure proper biogenesis of mature snoRNAs. However, one needs to consider cell-type-specific splicing patterns. For example, brain-specific Snord116 could only be efficiently expressed in a non-neuronal cell line upon mutating the wild-type 5′ splice site to the mammalian consensus motif (47,146). On the other hand, lack of (neuron-specific) splice factors alone cannot account for improper snoRNA biogenesis; for example, Snord116 and Snord115 were shown to be efficiently processed (although to a lesser extent) in numerous mouse non-neuronal tissues (e.g. lungs, heart, liver, spleen, kidney, muscle, testis and glial cells) upon induction of otherwise silenced host gene from maternal chromosome by knock-in of 5′*HPRT*-LoxP-*Neo*^{R} cassette upstream of the *Snord116* cluster (105).

In general, very few snoRNAs are essential for cell/organism viability, making it possible to resort to knock-out experiments, which are typically superior to studies based on knock-down approaches, as the latter may lead to incomplete or off-target effects. Due to its simplicity and convenience, CRISPR/Cas9 genome editing is being increasingly applied in snoRNA biology. For example, Vitali and Kiss (38) have used the technology to precisely delete the internal fragments of *EIF4G2* and *LARP4* gene introns harboring the SNORD97 and SCARNA97 genes, respectively, in order to support *in vivo* loss-of-function study in a near-haploid human cell line HAP1. In another example, Bochukova *et al.* (93) have used CRISPR/Cas9 genome editing to delete the 57.4 kb SNORD116 gene cluster from SH-SY5Y human neuroblastoma cells, thereby mimicking the PWS genotype. SH-SY5Y is a common cell model in neuroscience because it can easily be differentiated into mature neuron-like cells. Neuronal differentiation of SNORD116-deficient SH-SY5Y cells was reported to be impaired with cells displaying reduced initial proliferation and survival compared to wild-type cells, reminiscent of compromised brain development in Snord116 knock-out mice (94).

RNA modification analysis approaches

One of the earliest experimental methods for detecting canonical modifications (i.e. 2′-*O*-ribose methylation and pseudouridylation) exerted by snoRNPs on defined positions of presumed RNA targets was the primer extension assay (PEA). In PEA, reverse transcription is performed in the presence of increasing dNTP concentrations using a labeled primer annealing to the sequence downstream from the target site guided by a snoRNA. At low dNTP concentrations RNA modifications sterically hinder reverse transcriptase, causing it to stall, resulting in cDNA terminated at the nucleotide immediately before the modified site, whereas high dNTP concentrations rescue the RT processivity. Subjecting products of RT to high-resolution electrophoresis allows for identification of the modified site, and qPCR analysis of resulting cDNA can be used for quantifying the modification levels (127,133). Whereas ribose 2′-*O*-methylation efficiently slows down RT (147), pseudouridines can only be detected by first labeling (pseudo)uridine and guanidine residues with *N*-cyclohexyl-*N*′-beta-(4-methylmorpholinium)ethylcarbodiimide *p*-tosylate (CMC), followed by alkaline removal of all CMC groups except those linked to the N^3 of pseudouridine (148).

Similar principles can be exploited for high-throughput RNA modification analysis. Coupling CMC-treatment of RNA followed by selective alkaline adduct hydrolysis with RNA-seq provides means of transcriptome-wide quantitative mapping of pseudouridines (termed Ψ-seq) (149). Only some of the pseudouridylations are snoRNA-guided and catalyzed by dyskerin as judged from differential modifications observed in dyskerin knock-down/snoRNA knock-out and control yeast and mammalian cells. Interestingly, such modifications are not limited to rRNAs and snRNAs, and are also found in mRNAs and snoRNAs (149). RimSeq (4) is an unbiased high-throughput 2′-*O*-ribose methylation profiling technique based on compromised RT processivity at 2′-*O*-methylated sites at minute dNTP concentrations, and sequencing of prematurely terminated cDNAs. Inspecting 3′ ends of reads thus provides information on downstream methylation at single nucleotide resolution. Combining RimSeq with computational prediction of modified sites and literature data, Jorjani *et al.* (4) have proposed several previously undescribed snoRNA:rRNA/snRNA interactions, leaving only a small fraction of C/D-box snoRNAs orphan. Another approach, termed RiboMethSeq (150,151), relies on the fact that phosphodiester bond, located 3′ to a 2′-*O*-methylated residue, is protected from alkaline hydrolysis. Thus, partial fragmentation by random alkaline hydrolysis results in RNA segments beginning and ending at all sites, except at the nucleotide positioned directly downstream of the 2′-*O*-methyl carrying residue. Following RNA alkaline hydrolysis, deep sequencing is performed, and modified sites are called by 5′/3′ fragment end position counting. RiboMethSeq has been used to validate C/D-box snoRNA:target RNA interactions detected by CLIP (152) (see the *RNA:RNA interaction mapping* section below).

In addition to sequencing methods, mass spectrometry-based approaches for addressing RNA modifications have been reported, even for the 'mass-silent' pseudouridine (e.g. (153,154)). Although the latter are not considered high-throughput, they allow for identification of modifications inaccessible by sequencing, such as those found at the 3′ of RNA (leaving no room for reverse transcription primer binding in conventional methods) and the ones masked by adjacent modified residues. Furthermore, the indirect determination of modification sites in RNA is not immune to artefacts and the results should be treated with caution. In this regard, mass spectrometry approaches can be considered superior to indirect mapping of RNA modifications. For example, using the primer extension assay, Lacoux *et al*. (155) have reported that mouse BC1 RNA, a small non-

protein-coding RNA operating in the control of gene expression, is 2′-*O*-methylated at 5′-hairpin that is involved in mRNA translational regulation. On the other hand, targeted LC/MS analysis of native BC1 RNA found no base or sugar backbone modifications (156).

SnoRNA:protein interaction screening

SnoRNP dissection can provide clues as to snoRNA function. For example, identification of unexpected protein partners (considered components of non-canonical snoRNPs) strongly suggests an alternative role for that particular snoRNA, and this information can be used for subsequent mechanistic studies. On the other hand, a detailed analysis of (canonical) partner protein-associated snoRNAs can provide a glimpse into snoRNA biogenesis. snoRNA:protein interaction screening is typically based on targeted pull-down of snoRNPs, either using antibodies directed against specific proteins (i.e. RNA immunoprecipitation, RIP) or labeled antisense probes pairing to a certain segment of snoRNA (i.e. RNA antisense purification, RAP). Transient or weak direct protein:RNA interactions can be stabilized by ultraviolet (UVC) cross-linking in live cells, allowing for stringent purification conditions and ensuring that biologically relevant complexes are detected. Finally, proteins are identified by using mass spectrometry, and RNAs are subjected to sequencing.

RAP-MS (157,158) is especially appropriate for long RNAs as it relies on long (120 nt) biotinylated DNA antisense probes tiled along the length of entire targeted RNA. snoRNAs, on the other hand, are much shorter and, at least in canonical snoRNPs, heavily shielded by partner proteins. Targeting exposed snoRNA antisense elements might not be very efficient due to endogenous target RNA competition and inherently short length. Nevertheless, two groups report on successful snoRNP RAP experiments (24,80). In both cases, Snord115 was shown to interact with non-canonical protein partners, while interaction with fibrillarin could not be detected by MS. There was considerable overlap of the identified alternative protein partners, although distinct proteins were also detected in each study, which might be explained by employment of different probes (directed either against the ASE or the apical loop) and experimental conditions.

RIP (followed by microarray analysis or sequencing) is performed under native conditions, preserving RNA–protein association at the expense of specificity (159). Furthermore, it is incapable of capturing transient RNA:protein interactions. Thus, UV cross-linking and immunoprecipitation (CLIP) (160,161) and the closely related cross-linking and analysis of cDNAs (CRAC) (162,163) have become the methods of choice for identifying RNAs directly interacting with RNA-binding proteins (RBPs). Here, intact tissue or cells are irradiated with UVC light inducing covalent linkages between the RNAs and the closely associated proteins. In CLIP, cells are lysed, RNAs are partially fragmented by dilute RNase treatment, and the resulting fragments (protected by the partner protein) are co-immunoprecipitated with highly-specific antibodies under stringent purification conditions. A derivative technique called PAR-CLIP (photoactivatable ribonucleoside-enhanced CLIP (164)) exploits photoreactive nucleotide analogues incorporated in RNA during transcription to achieve more efficient cross-linking. CRAC differs from CLIP in that it uses an ectopically expressed RBP, terminally tagged with hexahistidine sequence, a protease cleavage site and protein A immunoglobulin binding domains. This allows for tandem RNP enrichment by first capturing RBP-RNA complexes on IgG beads under high salt conditions, and (following site-specific protease cleavage to release the complex) subsequent purification on Ni-NTA matrix under denaturing conditions. RNA pool linked to the RBP is labeled radioactively or with a fluorophore (via ligation of 5′ and 3′ adapters, respectively), subjected to SDS-PAGE, and transferred to nitrocellulose membrane in order to remove free RNA. Finally, piece of membrane with adsorbed complexes is cut out, RNA is released by proteinase K treatment, converted to cDNA and sequenced. Such methods have provided valuable insights into the architecture of canonical snoRNPs (163), and biogenesis and processing of snoRNAs (41). Fibrillarin RIP-seq screen was used to discover the SPAs and sno-lncRNAs of the PWS critical region (Figure 6) (83,117), and CLIP/CRAC-seq identified snoRNAs associating with unexpected protein partners (22,165).

A further improvement of the CLIP technique, the individual nucleotide-resolution UV cross-linking and immunoprecipitation (iCLIP) (166), is based on the fact that peptide/amino acid residue remaining cross-linked to RNA after proteinase K treatment will block RT. Thus, the cross-linking site is identified at the nucleotide +1 downstream to the cDNA terminus. RNA-seq library construction requires a modified approach, being based on ligating a 3′ universal adapter, serving as the RT primer annealing site, to RNA fragments, and then circularizing the resulting cDNA by using the single-stranded DNA ligase CircLigase to append a second universal sequence to the 3′ end for library PCR amplification.

RNA:RNA interaction mapping

RNA:RNA interaction mapping techniques are increasingly used for identifying targets of non-protein-coding RNAs. The approaches can be classified as *focused*, targeting one of the RNA partners or a specific RBP for enrichment of associated RNAs, or *unbiased*, allowing interrogation of the entire RNA interactome. The focused approaches are RAP-seq, CLIP, CLASH and hiCLIP, while the more recently developed unbiased methods include PARIS, SPLASH, LIGR-seq and COMRADES.

RAP-seq, similarly to RAP-MS discussed above, is based on tiled biotin-labeled antisense probes for selective pull-down of target RNA and its interacting partners. Once more, the size and compact structure of snoRNAs likely prohibits efficient RAP-seq. Engreitz *et al.* (167) described two variations of the method; in one direct RNA:RNA interactions are captured by a water-soluble photoreactive psoralen derivative 4′-aminomethyltrioxsalen (AMT) covalently cross-linking RNAs engaged in base pairing, while in the other indirect interactions mediated by proteins are stabilized via formaldehyde cross-linking. Conversely, specific protein components of RNPs can also be used

for RNA co-immunoprecipitation after UVC cross-linking and proximity ligation of interacting fragment RNA arms. Interestingly, even in sequencing data from conventional CLIP experiments, there have been reports of occasional hybrid reads, likely resulting from proximity ligation of two RNA fragments by endogenous ligases (127,152,168). To improve the ligation efficiency, RNA fragments cross-linked to a RBP can be specifically proximity ligated by T4 RNA ligase prior to library construction. Such techniques are CLASH (cross-linking, ligation, and sequencing of hybrids (33,169,170)) and hiCLIP (RNA hybrid and individual-nucleotide resolution ultraviolet cross-linking and immunoprecipitation (171,172)). HiCLIP differs from CLASH in that it uses an adapter that enables control over ligation of the two RNA arms comprising the RNA duplex, thereby overcoming the potential physical constraints of the ligation reaction. Importantly, it also enables each arm of the duplex to be unambiguously identified during bioinformatic analysis of sequencing data, ensuring that both intra- and intermolecular RNA-RNA interactions are precisely defined on transcripts. Fibrillarin/Nop56/Nop58-CLASH has been extensively used for validation of snoRNA targets in yeast (33,169).

Whereas CLASH and (hi)CLIP are limited by the choice of RBP for purifying RNA:RNA duplexes as well as by the likely underrepresentation of transient RNA:RNA interactions in the final sequencing library, recent state-of-the-art methods of RNA interactome profiling allow for unbiased transcriptome-wide RNA:RNA interaction identification. All are similar in that they rely on psoralen derivatives to stabilize cellular RNA:RNA interactions, but differ in the way the cross-linked RNA duplexes are enriched prior to hybrid RNA library construction. In LIGR-seq (ligation of interacting RNA followed by high-throughput sequencing (48)) cells are incubated with AMT and irradiated by UVA light, and RNA is Trizol-extracted. Next, sample is treated with S1 nuclease which cleaves single-stranded but not double-stranded RNA, and heat-denatured. Cross-linked RNA fragments are proximity ligated, and treated with RNase R, a 3′→5′ exoribonuclease that degrades essentially all linear RNAs but does not digest lariat or circular RNA structures, effectively enriching hybrids. In PARIS (psoralen analysis of RNA interactions and structures (34,173)) S1 nuclease/RNase III-fragmented AMT-cross-linked RNA is subjected to 2D electrophoresis. Initially, RNA is separated on native polyacrylamide gel and size-selected according to presumed double-stranded structure (e.g. 25–150 bp). Gel slices from the first dimension are then embedded perpendicularly on a high-resolution denaturing polyacrylamide gel, and run at high voltage to induce heat. Upon gel staining, denatured cross-linked RNA emerges above the main diagonal, and can be extracted for subsequent proximity ligation. SPLASH (sequencing of psoralen-crosslinked, ligated, and selected hybrids (174)) employs a biotinylated psoralen for RNA cross-linking, followed by capture of Mg^{2+}-fragmented cross-linked RNA segments on streptavidin beads, and proximity ligation. Biotinylated psoralen entry into cells is very inefficient, and cells need to be incubated with a detergent (0.01% digitonin) to improve intracellular delivery. However, any additional stress exerted to cells during the lengthy cross-linking step might perturb the RNA interactome. In this regard, COMRADES (cross-linking of matched RNAs and deep sequencing (175)) is a markedly improved technique, based on cross-linking RNA with a cell-permeable azide-modified psoralen derivative (psoralen-triethylene glycol azide). Trizol-extracted RNase III-fragmented RNA is reacted with an alkyne-containing click reagent carrying a biotin moiety for quantitative labeling of cross-linked RNA fragments, allowing streptavidin capture. Following proximity ligation, psoralene-induced cross-links are easily reversed by irradiation with UVC light, and hybrid RNA sequencing libraries can be generated using standard methods. Methods for RNA:RNA interaction mapping have been used to confirm presumed targets of snoRNAs as well as identify new non-canonical ones (34,48,152,173,174).

Induced pluripotent stem cell models in snoRNA functional analysis

Knock-down and knock-out technologies are vital tools for comparative transcriptome and phenotype analyses (relative to wild-type cells and animals), however, cell models based on actual patient genotypes are often preferable. The ability to dedifferentiate any somatic cell to the level of pluripotency has opened a new and exciting field in the study of genetic diseases, including those directly or indirectly linked to snoRNAs. Reprogramming of patient-derived cells, usually fibroblasts obtained from skin biopsy, involves transfection or transduction with a handful of embryonic transcription factors and/or miRNAs (176,177). Resulting induced pluripotent stem cells (iPSC) can propagate indefinitely and can be differentiated to various disease-relevant cell types *in vitro*. With relevance to snoRNA biology, iPSC from PWS subjects (178–180) and patients with X-linked form of dyskeratosis congenita (X-DC; caused by mutation in the dyskerin gene) (181,182) have been generated. DC is a congenital bone marrow failure syndrome, further clinically characterized by reticular skin pigmentation, nail dystrophy, and mucosal leukoplakia. Indicating that iPSCs provide relevant disease models are the notions that PWS iPSC-derived neurons retain the molecular signature of PWS (i.e. maternal genes from the PWS remained silenced in iPSCs and typical DNA methylation patterns persisted all through neuronal differentiation (178)), and that X-DC iPSCs show noticeable reduction in telomerase activity, progressively affecting iPSC self-renewal (182). The latter can be attributed to the vital role of dyskerin in telomerase RNP assembly and localization (183), as the telomerase RNA component (TERC) contains a 3′ terminal domain resembling H/ACA-box snoRNA.

CONCLUSIONS AND OUTLOOK

RNAs, despite being structurally fairly simple molecules, display extraordinary functional flexibility, which seems to be true also for snoRNAs. In addition to well-defined roles in guiding 2′-*O* ribose methylation and pseudouridylation on rRNA and snRNA targets, individual snoRNAs were implicated in governing mRNA abundance by what seem to be complex mechanisms, regulation of RNA splicing, and

directing an unexpected type of post-transcriptional modification (i.e., cytosine N^4 acetylation). With regards to snoRNAs' modes of action, it may well be that we have only been picking the low-hanging fruit. Indeed, given the pace of field development, it is likely that the list of unexpected snoRNA roles will further expand. New state-of-the-art methods enabling insights into alternative snoRNP composition, direct target identification, and detection of RNA modifications at a transcriptome-wide level provide a snoRNA biology research toolbox of unprecedented power. Yet, functional characterization of snoRNA might be hampered by several factors, such as technical limitations of analytical methods, intrinsic snoRNA properties, potential dual (multiple?) functionalities of snoRNAs, and functional heterogeneity of snoRNA-expressing tissues. For example, compact folding, protection by partner proteins, small size and competition with endogenous target RNAs decrease efficiency of antisense-based snoRNPs purification, especially if their expression levels are low. Furthermore, structural complexity may limit the efficiency of reverse transcription reactions for subsets of RNAs (or RNA hybrids) prior to construction of RNA-seq library, skewing the transcriptome/RNA interactome profiling. Novel protocols based on the robust thermostable group II intron reverse transcriptases (TGIRTs) are being developed to overcome the issue of limited RT processivity and to increase coverage in RNA-seq experiments (e.g. (184)). Another exciting field in RNA biology is single-cell RNA-seq (185), a rapidly expanding technology allowing the dissection of gene expression at single-cell resolution. This approach is especially appealing in characterization of heterogeneous tissues, such as brain, where bulk sequencing might mask intricate cell-type differences. Given the limited expression profiles of certain orphan snoRNAs (e.g. (111,134)), we expect that single-cell RNA-seq will play a major role in snoRNA functional analyses in the future. Current single-cell RNA-seq approaches already support a wide variety of applications; among others identification of cell subpopulations, detection of rare cell states, differential gene expression analysis, analysis of splicing and RNA editing, and developmental trajectories reconstruction (185,186). Although currently single-cell RNA-seq data are more complex and 'noisier' compared to conventional bulk RNA-seq data, experimental protocols allowing transcriptome capture with higher sensitivity are continuously being designed, and improved computational platforms are being developed to cope with data analysis (reviewed in (187)). Modern single-cell omic technologies take a step further, and attempt to address different aspects of gene expression (e.g. transcriptome and proteome analysis) simultaneously. One such example, termed CITE-seq (cellular indexing of transcriptomes and epitopes by sequencing (188)) takes advantage of oligonucleotide barcode-tagged antibodies specific for cell surface proteins to measure protein abundance via sequencing (the barcode frequency reflects the relative protein concentration) at single-cell resolution concomitantly with transcriptome profiling. On the other hand, bioinformatic platforms integrating transcriptome-wide RNA structural analysis with post-transcriptional modification profiling (collectively termed *RNA epistructurome* (189)) from the same set of NGS-based data are being developed to help users tackle the problem of RNA functional characterization (190).

FUNDING

Slovenian Research Agency [P4-0127, J3-9263]; Foundation for Prader-Willi Research. Funding for open access charge: Javna Agencija za Raziskovalno Dejavnost RS.
Conflict of interest statement. None declared.

REFERENCES

1. Dieci,G., Preti,M. and Montanini,B. (2009) Eukaryotic snoRNAs: a paradigm for gene expression flexibility. *Genomics*, **94**, 83–88.
2. Bratkovič,T. and Rogelj,B. (2011) Biology and applications of small nucleolar RNAs. *Cell Mol. Life Sci.*, **68**, 3843–3851.
3. Tollervey,D. and Kiss,T. (1997) Function and synthesis of small nucleolar RNAs. *Curr. Opin. Cell Biol.*, **9**, 337–342.
4. Jorjani,H., Kehr,S., Jedlinski,D.J., Gumienny,R., Hertel,J., Stadler,P.F., Zavolan,M. and Gruber,A.R. (2016) An updated human snoRNAome. *Nucleic Acids Res.*, **44**, 5068–5082.
5. Kiss-Laszlo,Z., Henry,Y., Bachellerie,J.P., Caizergues-Ferrer,M. and Kiss,T. (1996) Site-specific ribose methylation of preribosomal RNA: a novel function for small nucleolar RNAs. *Cell*, **85**, 1077–1088.
6. Yu,G., Zhao,Y. and Li,H. (2018) The multistructural forms of box C/D ribonucleoprotein particles. *RNA*, **24**, 1625–1633.
7. Weinstein Szewczak,L.B., DeGregorio,S.J., Strobel,S.A. and Steitz,J.A. (2002) Exclusive interaction of the 15.5 kD protein with the terminal box C/D motif of a methylation guide snoRNP. *Chem. Biol.*, **9**, 1095–1107.
8. Kiss,A.M., Jady,B.E., Bertrand,E. and Kiss,T. (2004) Human box H/ACA pseudouridylation guide RNA machinery. *Mol. Cell Biol.*, **24**, 5797–5807.
9. Bohnsack,M.T. and Sloan,K.E. (2018) Modifications in small nuclear RNAs and their roles in spliceosome assembly and function. *Biol. Chem.*, **399**, 1265–1276.
10. Sloan,K.E., Warda,A.S., Sharma,S., Entian,K.D., Lafontaine,D.L.J. and Bohnsack,M.T. (2017) Tuning the ribosome: the influence of rRNA modification on eukaryotic ribosome biogenesis and function. *RNA Biol.*, **14**, 1138–1152.
11. Karijolich,J., Kantartzis,A. and Yu,Y.T. (2010) RNA modifications: a mechanism that modulates gene expression. *Methods Mol. Biol.*, **629**, 1–19.
12. Henras,A.K., Plisson-Chastang,C., Humbert,O., Romeo,Y. and Henry,Y. (2017) Synthesis, function, and heterogeneity of snoRNA-guided posttranscriptional nucleoside modifications in eukaryotic ribosomal RNAs. *Enzymes*, **41**, 169–213.
13. Yang,Z., Lin,J. and Ye,K. (2016) Box C/D guide RNAs recognize a maximum of 10 nt of substrates. *Proc. Natl. Acad. Sci. U.S.A.*, **113**, 10878–10883.
14. Lin,J., Lai,S., Jia,R., Xu,A., Zhang,L., Lu,J. and Ye,K. (2011) Structural basis for site-specific ribose methylation by box C/D RNA protein complexes. *Nature*, **469**, 559–563.
15. Duan,J., Li,L., Lu,J., Wang,W. and Ye,K. (2009) Structural mechanism of substrate RNA recruitment in H/ACA RNA-guided pseudouridine synthase. *Mol. Cell*, **34**, 427–439.
16. Dragon,F., Gallagher,J.E., Compagnone-Post,P.A., Mitchell,B.M., Porwancher,K.A., Wehner,K.A., Wormsley,S., Settlage,R.E., Shabanowitz,J., Osheim,Y. *et al.* (2002) A large nucleolar U3 ribonucleoprotein required for 18S ribosomal RNA biogenesis. *Nature*, **417**, 967–970.
17. Tycowski,K.T., Shu,M.D. and Steitz,J.A. (1994) Requirement for intron-encoded U22 small nucleolar RNA in 18S ribosomal RNA maturation. *Science*, **266**, 1558–1561.
18. Peculis,B.A. and Steitz,J.A. (1993) Disruption of U8 nucleolar snRNA inhibits 5.8S and 28S rRNA processing in the Xenopus oocyte. *Cell*, **73**, 1233–1245.
19. Fayet-Lebaron,E., Atzorn,V., Henry,Y. and Kiss,T. (2009) 18S rRNA processing requires base pairings of snR30 H/ACA snoRNA to eukaryote-specific 18S sequences. *EMBO J.*, **28**, 1260–1270.

20. Deryusheva,S. and Gall,J.G. (2019) scaRNAs and snoRNAs: are they limited to specific classes of substrate RNAs? *RNA*, **25**, 17–22.
21. Falaleeva,M., Pages,A., Matuszek,Z., Hidmi,S., Agranat-Tamir,L., Korotkov,K., Nevo,Y., Eyras,E., Sperling,R. and Stamm,S. (2016) Dual function of C/D box small nucleolar RNAs in rRNA modification and alternative pre-mRNA splicing. *Proc. Natl. Acad. Sci. U.S.A.*, **113**, E1625–E1634.
22. Sharma,S., Yang,J., van Nues,R., Watzinger,P., Kotter,P., Lafontaine,D.L.J., Granneman,S. and Entian,K.D. (2017) Specialized box C/D snoRNPs act as antisense guides to target RNA base acetylation. *PLoS Genet.*, **13**, e1006804.
23. Huang,C., Shi,J., Guo,Y., Huang,W., Huang,S., Ming,S., Wu,X., Zhang,R., Ding,J., Zhao,W. *et al.* (2017) A snoRNA modulates mRNA 3′ end processing and regulates the expression of a subset of mRNAs. *Nucleic Acids Res.*, **45**, 8647–8660.
24. Soeno,Y., Taya,Y., Stasyk,T., Huber,L.A., Aoba,T. and Huttenhofer,A. (2010) Identification of novel ribonucleo-protein complexes from the brain-specific snoRNA MBII-52. *RNA*, **16**, 1293–1300.
25. Rogelj,B. (2006) Brain-specific small nucleolar RNAs. *J. Mol. Neurosci.*, **28**, 103–109.
26. Cavaille,J., Buiting,K., Kiefmann,M., Lalande,M., Brannan,C.I., Horsthemke,B., Bachellerie,J.P., Brosius,J. and Huttenhofer,A. (2000) Identification of brain-specific and imprinted small nucleolar RNA genes exhibiting an unusual genomic organization. *Proc. Natl. Acad. Sci. U.S.A.*, **97**, 14311–14316.
27. Yang,J.H., Zhang,X.C., Huang,Z.P., Zhou,H., Huang,M.B., Zhang,S., Chen,Y.Q. and Qu,L.H. (2006) snoSeeker: an advanced computational package for screening of guide and orphan snoRNA genes in the human genome. *Nucleic Acids Res.*, **34**, 5112–5123.
28. Hertel,J., Hofacker,I.L. and Stadler,P.F. (2008) SnoReport: computational identification of snoRNAs with unknown targets. *Bioinformatics*, **24**, 158–164.
29. de Araujo Oliveira,J.V., Costa,F., Backofen,R., Stadler,P.F., Machado Telles Walter,M.E. and Hertel,J. (2016) SnoReport 2.0: new features and a refined support vector machine to improve snoRNA identification. *BMC Bioinformatics*, **17**, 464.
30. Helm,M. and Motorin,Y. (2017) Detecting RNA modifications in the epitranscriptome: predict and validate. *Nat. Rev. Genet.*, **18**, 275–291.
31. El Yacoubi,B., Bailly,M. and de Crecy-Lagard,V. (2012) Biosynthesis and function of posttranscriptional modifications of transfer RNAs. *Annu. Rev. Genet.*, **46**, 69–95.
32. Walkley,C.R. and Li,J.B. (2017) Rewriting the transcriptome: adenosine-to-inosine RNA editing by ADARs. *Genome Biol.*, **18**, 205.
33. Dudnakova,T., Dunn-Davies,H., Peters,R. and Tollervey,D. (2018) Mapping targets for small nucleolar RNAs in yeast. *Wellcome Open Res*, **3**, 120.
34. Lu,Z., Zhang,Q.C., Lee,B., Flynn,R.A., Smith,M.A., Robinson,J.T., Davidovich,C., Gooding,A.R., Goodrich,K.J., Mattick,J.S. *et al.* (2016) RNA duplex map in living cells reveals higher-order transcriptome structure. *Cell*, **165**, 1267–1279.
35. Sharma,S., Langhendries,J.L., Watzinger,P., Kotter,P., Entian,K.D. and Lafontaine,D.L. (2015) Yeast Kre33 and human NAT10 are conserved 18S rRNA cytosine acetyltransferases that modify tRNAs assisted by the adaptor Tan1/THUMPD1. *Nucleic Acids Res.*, **43**, 2242–2258.
36. Jackman,J.E. and Alfonzo,J.D. (2013) Transfer RNA modifications: nature's combinatorial chemistry playground. *Wiley Interdiscip. Rev. RNA*, **4**, 35–48.
37. Dennis,P.P. and Omer,A. (2005) Small non-coding RNAs in Archaea. *Curr. Opin. Microbiol.*, **8**, 685–694.
38. Vitali,P. and Kiss,T. (2019) Cooperative 2′-O-methylation of the wobble cytidine of human elongator tRNA(Met)(CAT) by a nucleolar and a Cajal body-specific box C/D RNP. *Genes Dev.*, **33**, 741–746.
39. Yamasaki,S., Ivanov,P., Hu,G.F. and Anderson,P. (2009) Angiogenin cleaves tRNA and promotes stress-induced translational repression. *J. Cell Biol.*, **185**, 35–42.
40. Ivanov,P., Emara,M.M., Villen,J., Gygi,S.P. and Anderson,P. (2011) Angiogenin-induced tRNA fragments inhibit translation initiation. *Mol. Cell*, **43**, 613–623.
41. Kishore,S., Gruber,A.R., Jedlinski,D.J., Syed,A.P., Jorjani,H. and Zavolan,M. (2013) Insights into snoRNA biogenesis and processing from PAR-CLIP of snoRNA core proteins and small RNA sequencing. *Genome Biol.*, **14**, R45.
42. Zemann,A., op de Bekke,A., Kiefmann,M., Brosius,J. and Schmitz,J. (2006) Evolution of small nucleolar RNAs in nematodes. *Nucleic Acids Res.*, **34**, 2676–2685.
43. Shi,Y. and Manley,J.L. (2015) The end of the message: multiple protein-RNA interactions define the mRNA polyadenylation site. *Genes Dev.*, **29**, 889–897.
44. Shi,J., Huang,C., Huang,S. and Yao,C. (2018) snoRNAs associate with mRNA 3′ processing complex: New wine in old bottles. *RNA Biol.*, **15**, 194–197.
45. Romano,G., Veneziano,D., Acunzo,M. and Croce,C.M. (2017) Small non-coding RNA and cancer. *Carcinogenesis*, **38**, 485–491.
46. Abel,Y. and Rederstorff,M. (2019) SnoRNAs and the emerging class of sdRNAs: multifaceted players in oncogenesis. *Biochimie*, **164**, 17–21.
47. Falaleeva,M., Surface,J., Shen,M., de la Grange,P. and Stamm,S. (2015) SNORD116 and SNORD115 change expression of multiple genes and modify each other's activity. *Gene*, **572**, 266–273.
48. Sharma,E., Sterne-Weiler,T., O'Hanlon,D. and Blencowe,B.J. (2016) Global mapping of human RNA-RNA interactions. *Mol. Cell*, **62**, 618–626.
49. Taft,R.J., Glazov,E.A., Lassmann,T., Hayashizaki,Y., Carninci,P. and Mattick,J.S. (2009) Small RNAs derived from snoRNAs. *RNA*, **15**, 1233–1240.
50. Brameier,M., Herwig,A., Reinhardt,R., Walter,L. and Gruber,J. (2011) Human box C/D snoRNAs with miRNA like functions: expanding the range of regulatory RNAs. *Nucleic. Acids. Res.*, **39**, 675–686.
51. Martens-Uzunova,E.S., Olvedy,M. and Jenster,G. (2013) Beyond microRNA–novel RNAs derived from small non-coding RNA and their implication in cancer. *Cancer Lett.*, **340**, 201–211.
52. Scott,M.S. and Ono,M. (2011) From snoRNA to miRNA: dual function regulatory non-coding RNAs. *Biochimie*, **93**, 1987–1992.
53. Falaleeva,M. and Stamm,S. (2013) Processing of snoRNAs as a new source of regulatory non-coding RNAs: snoRNA fragments form a new class of functional RNAs. *Bioessays*, **35**, 46–54.
54. Shen,M., Eyras,E., Wu,J., Khanna,A., Josiah,S., Rederstorff,M., Zhang,M.Q. and Stamm,S. (2011) Direct cloning of double-stranded RNAs from RNase protection analysis reveals processing patterns of C/D box snoRNAs and provides evidence for widespread antisense transcript expression. *Nucleic Acids Res.*, **39**, 9720–9730.
55. Scott,M.S., Ono,M., Yamada,K., Endo,A., Barton,G.J. and Lamond,A.I. (2012) Human box C/D snoRNA processing conservation across multiple cell types. *Nucleic Acids Res.*, **40**, 3676–3688.
56. Ono,M., Scott,M.S., Yamada,K., Avolio,F., Barton,G.J. and Lamond,A.I. (2011) Identification of human miRNA precursors that resemble box C/D snoRNAs. *Nucleic Acids Res.*, **39**, 3879–3891.
57. Thomson,D.W., Pillman,K.A., Anderson,M.L., Lawrence,D.M., Toubia,J., Goodall,G.J. and Bracken,C.P. (2015) Assessing the gene regulatory properties of Argonaute-bound small RNAs of diverse genomic origin. *Nucleic Acids Res.*, **43**, 470–481.
58. Ender,C., Krek,A., Friedlander,M.R., Beitzinger,M., Weinmann,L., Chen,W., Pfeffer,S., Rajewsky,N. and Meister,G. (2008) A human snoRNA with microRNA-like functions. *Mol. Cell*, **32**, 519–528.
59. Li,W., Saraiya,A.A. and Wang,C.C. (2011) Gene regulation in *Giardia lambia* involves a putative microRNA derived from a small nucleolar RNA. *PLoS Negl. Trop. Dis.*, **5**, e1338.
60. Ono,M., Yamada,K., Avolio,F., Scott,M.S., van Koningsbruggen,S., Barton,G.J. and Lamond,A.I. (2010) Analysis of human small nucleolar RNAs (snoRNA) and the development of snoRNA modulator of gene expression vectors. *Mol. Biol. Cell*, **21**, 1569–1584.
61. Tomlinson,D.C., L'Hote,C.G., Kennedy,W., Pitt,E. and Knowles,M.A. (2005) Alternative splicing of fibroblast growth factor receptor 3 produces a secreted isoform that inhibits fibroblast growth factor-induced proliferation and is repressed in urothelial carcinoma cell lines. *Cancer Res.*, **65**, 10441–10449.

62. Lorenz,R., Bernhart,S.H., Honer Zu Siederdissen,C., Tafer,H., Flamm,C., Stadler,P.F. and Hofacker,I.L. (2011) ViennaRNA Package 2.0. *Algorithms Mol. Biol.*, **6**, 26.
63. Ono,M., Yamada,K., Bensaddek,D., Afzal,V., Biddlestone,J., Ortmann,B., Mudie,S., Boivin,V., Scott,M.S., Rocha,S. *et al.* (2016) Enhanced snoMEN vectors facilitate establishment of GFP-HIF-1alpha protein replacement human cell lines. *PLoS One*, **11**, e0154759.
64. Ono,M., Yamada,K., Avolio,F., Afzal,V., Bensaddek,D. and Lamond,A.I. (2015) Targeted knock-down of miR21 primary transcripts using snoMEN vectors induces apoptosis in human cancer cell lines. *PLoS One*, **10**, e0138668.
65. Ono,M., Yamada,K., Endo,A., Avolio,F. and Lamond,A.I. (2013) Analysis of human protein replacement stable cell lines established using snoMEN-PR vector. *PLoS One*, **8**, e62305.
66. Das,U., Nguyen,H. and Xie,J. (2019) Transcriptome protection by the expanded family of hnRNPs. *RNA Biol.*, **16**, 155–159.
67. Stepanov,G.A., Semenov,D.V., Kuligina,E.V., Koval,O.A., Rabinov,I.V., Kit,Y.Y. and Richter,V.A. (2012) Analogues of artificial human box C/D small nucleolar RNA as regulators of alternative splicing of a pre-mRNA target. *Acta Naturae*, **4**, 32–41.
68. Stepanov,G.A., Semenov,D.V., Savelyeva,A.V., Kuligina,E.V., Koval,O.A., Rabinov,I.V. and Richter,V.A. (2013) Artificial box C/D RNAs affect pre-mRNA maturation in human cells. *Biomed. Res. Int.*, **2013**, 656158.
69. Zhang,Y.J., Yang,J.H., Shi,Q.S., Zheng,L.L., Liu,J., Zhou,H., Zhang,H. and Qu,L.H. (2014) Rapid birth-and-death evolution of imprinted snoRNAs in the Prader-Willi syndrome locus: implications for neural development in Euarchontoglires. *PLoS One*, **9**, e100329.
70. Chen,C.L., Perasso,R., Qu,L.H. and Amar,L. (2007) Exploration of pairing constraints identifies a 9 base-pair core within box C/D snoRNA-rRNA duplexes. *J. Mol. Biol.*, **369**, 771–783.
71. Burns,C.M., Chu,H., Rueter,S.M., Hutchinson,L.K., Canton,H., Sanders-Bush,E. and Emeson,R.B. (1997) Regulation of serotonin-2C receptor G-protein coupling by RNA editing. *Nature*, **387**, 303–308.
72. Niswender,C.M., Copeland,S.C., Herrick-Davis,K., Emeson,R.B. and Sanders-Bush,E. (1999) RNA editing of the human serotonin 5-hydroxytryptamine 2C receptor silences constitutive activity. *J. Biol. Chem.*, **274**, 9472–9478.
73. Price,R.D., Weiner,D.M., Chang,M.S. and Sanders-Bush,E. (2001) RNA editing of the human serotonin 5-HT2C receptor alters receptor-mediated activation of G13 protein. *J. Biol. Chem.*, **276**, 44663–44668.
74. Zhang,Z., Shen,M., Gresch,P.J., Ghamari-Langroudi,M., Rabchevsky,A.G., Emeson,R.B. and Stamm,S. (2016) Oligonucleotide-induced alternative splicing of serotonin 2C receptor reduces food intake. *EMBO Mol. Med.*, **8**, 878–894.
75. Flomen,R., Knight,J., Sham,P., Kerwin,R. and Makoff,A. (2004) Evidence that RNA editing modulates splice site selection in the 5-HT2C receptor gene. *Nucleic Acids Res.*, **32**, 2113–2122.
76. Martin,C.B., Ramond,F., Farrington,D.T., Aguiar,A.S. Jr., Chevarin,C., Berthiau,A.S., Caussanel,S., Lanfumey,L., Herrick-Davis,K., Hamon,M. *et al.* (2013) RNA splicing and editing modulation of 5-HT(2C) receptor function: relevance to anxiety and aggression in VGV mice. *Mol. Psychiatry*, **18**, 656–665.
77. Kishore,S. and Stamm,S. (2006) The snoRNA HBII-52 regulates alternative splicing of the serotonin receptor 2C. *Science*, **311**, 230–232.
78. Bratkovič,T., Modic,M., Camargo Ortega,G., Drukker,M. and Rogelj,B. (2018) Neuronal differentiation induces SNORD115 expression and is accompanied by post-transcriptional changes of serotonin receptor 2c mRNA. *Sci. Rep.*, **8**, 5101.
79. Raabe,C.A., Voss,R., Kummerfeld,D.M., Brosius,J., Galiveti,C.R., Wolters,A., Seggewiss,J., Huge,A., Skryabin,B.V. and Rozhdestvensky,T.S. (2019) Ectopic expression of Snord115 in choroid plexus interferes with editing but not splicing of 5-Ht2c receptor pre-mRNA in mice. *Sci. Rep.*, **9**, 4300.
80. Kishore,S., Khanna,A., Zhang,Z., Hui,J., Balwierz,P.J., Stefan,M., Beach,C., Nicholls,R.D., Zavolan,M. and Stamm,S. (2010) The snoRNA MBII-52 (SNORD 115) is processed into smaller RNAs and regulates alternative splicing. *Hum. Mol. Genet.*, **19**, 1153–1164.
81. Lykke-Andersen,S., Chen,Y., Ardal,B.R., Lilje,B., Waage,J., Sandelin,A. and Jensen,T.H. (2014) Human nonsense-mediated RNA decay initiates widely by endonucleolysis and targets snoRNA host genes. *Genes Dev.*, **28**, 2498–2517.
82. Lykke-Andersen,S., Ardal,B.K., Hollensen,A.K., Damgaard,C.K. and Jensen,T.H. (2018) Box C/D snoRNP autoregulation by a cis-acting snoRNA in the NOP56 pre-mRNA. *Mol. Cell*, **72**, 99–111.
83. Wu,H., Yin,Q.F., Luo,Z., Yao,R.W., Zheng,C.C., Zhang,J., Xiang,J.F., Yang,L. and Chen,L.L. (2016) Unusual processing generates SPA lncRNAs that sequester multiple RNA binding proteins. *Mol. Cell*, **64**, 534–548.
84. Kocher,M.A. and Good,D.J. (2017) Phylogenetic analysis of the SNORD116 locus. *Genes (Basel)*, **8**, E358.
85. Angulo,M.A., Butler,M.G. and Cataletto,M.E. (2015) Prader-Willi syndrome: a review of clinical, genetic, and endocrine findings. *J. Endocrinol. Invest.*, **38**, 1249–1263.
86. Fountain,M.D., Aten,E., Cho,M.T., Juusola,J., Walkiewicz,M.A., Ray,J.W., Xia,F., Yang,Y., Graham,B.H., Bacino,C.A. *et al.* (2017) The phenotypic spectrum of Schaaf-Yang syndrome: 18 new affected individuals from 14 families. *Genet. Med.*, **19**, 45–52.
87. Schaaf,C.P., Gonzalez-Garay,M.L., Xia,F., Potocki,L., Gripp,K.W., Zhang,B., Peters,B.A., McElwain,M.A., Drmanac,R., Beaudet,A.L. *et al.* (2013) Truncating mutations of MAGEL2 cause Prader-Willi phenotypes and autism. *Nat. Genet.*, **45**, 1405–1408.
88. Cavaille,J. (2017) Box C/D small nucleolar RNA genes and the Prader-Willi syndrome: a complex interplay. *Wiley Interdiscip. Rev. RNA*, **8**, e1417.
89. de Smith,A.J., Purmann,C., Walters,R.G., Ellis,R.J., Holder,S.E., Van Haelst,M.M., Brady,A.F., Fairbrother,U.L., Dattani,M., Keogh,J.M. *et al.* (2009) A deletion of the HBII-85 class of small nucleolar RNAs (snoRNAs) is associated with hyperphagia, obesity and hypogonadism. *Hum. Mol. Genet.*, **18**, 3257–3265.
90. Duker,A.L., Ballif,B.C., Bawle,E.V., Person,R.E., Mahadevan,S., Alliman,S., Thompson,R., Traylor,R., Bejjani,B.A., Shaffer,L.G. *et al.* (2010) Paternally inherited microdeletion at 15q11.2 confirms a significant role for the SNORD116 C/D box snoRNA cluster in Prader-Willi syndrome. *Eur. J. Hum. Genet.*, **18**, 1196–1201.
91. Bieth,E., Eddiry,S., Gaston,V., Lorenzini,F., Buffet,A., Conte Auriol,F., Molinas,C., Cailley,D., Rooryck,C., Arveiler,B. *et al.* (2015) Highly restricted deletion of the SNORD116 region is implicated in Prader-Willi Syndrome. *Eur. J. Hum. Genet.*, **23**, 252–255.
92. Sahoo,T., del Gaudio,D., German,J.R., Shinawi,M., Peters,S.U., Person,R.E., Garnica,A., Cheung,S.W. and Beaudet,A.L. (2008) Prader-Willi phenotype caused by paternal deficiency for the HBII-85 C/D box small nucleolar RNA cluster. *Nat. Genet.*, **40**, 719–721.
93. Bochukova,E.G., Lawler,K., Croizier,S., Keogh,J.M., Patel,N., Strohbehn,G., Lo,K.K., Humphrey,J., Hokken-Koelega,A., Damen,L. *et al.* (2018) A transcriptomic signature of the hypothalamic response to fasting and BDNF deficiency in Prader-Willi syndrome. *Cell Rep.*, **22**, 3401–3408.
94. Burnett,L.C., Hubner,G., LeDuc,C.A., Morabito,M.V., Carli,J.F.M. and Leibel,R.L. (2017) Loss of the imprinted, non-coding Snord116 gene cluster in the interval deleted in the Prader Willi syndrome results in murine neuronal and endocrine pancreatic developmental phenotypes. *Hum. Mol. Genet.*, **26**, 4606–4616.
95. Adhikari,A., Copping,N.A., Onaga,B., Pride,M.C., Coulson,R.L., Yang,M., Yasui,D.H., LaSalle,J.M. and Silverman,J.L. (2019) Cognitive deficits in the Snord116 deletion mouse model for Prader-Willi syndrome. *Neurobiol. Learn. Mem.*, **165**, 106874.
96. Meguro,M., Mitsuya,K., Nomura,N., Kohda,M., Kashiwagi,A., Nishigaki,R., Yoshioka,H., Nakao,M., Oishi,M. and Oshimura,M. (2001) Large-scale evaluation of imprinting status in the Prader-Willi syndrome region: an imprinted direct repeat cluster resembling small nucleolar RNA genes. *Hum. Mol. Genet.*, **10**, 383–394.
97. de los Santos,T., Schweizer,J., Rees,C.A. and Francke,U. (2000) Small evolutionarily conserved RNA, resembling C/D box small nucleolar RNA, is transcribed from PWCR1, a novel imprinted gene in the Prader-Willi deletion region, which Is highly expressed in brain. *Am. J. Hum. Genet.*, **67**, 1067–1082.
98. Bervini,S. and Herzog,H. (2013) Mouse models of Prader-Willi Syndrome: a systematic review. *Front. Neuroendocrinol.*, **34**, 107–119.

99. Rodriguez,J.A. and Zigman,J.M. (2018) Hypothalamic loss of Snord116 and Prader-Willi syndrome hyperphagia: the buck stops here? *J. Clin. Invest.*, **128**, 900–902.
100. Relkovic,D. and Isles,A.R. (2013) Behavioural and cognitive profiles of mouse models for Prader-Willi syndrome. *Brain Res. Bull.*, **92**, 41–48.
101. Vitali,P., Royo,H., Marty,V., Bortolin-Cavaille,M.L. and Cavaille,J. (2010) Long nuclear-retained non-coding RNAs and allele-specific higher-order chromatin organization at imprinted snoRNA gene arrays. *J. Cell Sci.*, **123**, 70–83.
102. Powell,W.T., Coulson,R.L., Gonzales,M.L., Crary,F.K., Wong,S.S., Adams,S., Ach,R.A., Tsang,P., Yamada,N.A., Yasui,D.H. *et al.* (2013) R-loop formation at Snord116 mediates topotecan inhibition of Ube3a-antisense and allele-specific chromatin decondensation. *Proc. Natl. Acad. Sci. U.S.A.*, **110**, 13938–13943.
103. Powell,W.T., Coulson,R.L., Crary,F.K., Wong,S.S., Ach,R.A., Tsang,P., Alice Yamada,N., Yasui,D.H. and Lasalle,J.M. (2013) A Prader-Willi locus lncRNA cloud modulates diurnal genes and energy expenditure. *Hum. Mol. Genet.*, **22**, 4318–4328.
104. Ding,F., Li,H.H., Zhang,S., Solomon,N.M., Camper,S.A., Cohen,P. and Francke,U. (2008) SnoRNA Snord116 (Pwcr1/MBII-85) deletion causes growth deficiency and hyperphagia in mice. *PLoS One*, **3**, e1709.
105. Rozhdestvensky,T.S., Robeck,T., Galiveti,C.R., Raabe,C.A., Seeger,B., Wolters,A., Gubar,L.V., Brosius,J. and Skryabin,B.V. (2016) Maternal transcription of non-protein coding RNAs from the PWS-critical region rescues growth retardation in mice. *Sci. Rep.*, **6**, 20398.
106. Skryabin,B.V., Gubar,L.V., Seeger,B., Pfeiffer,J., Handel,S., Robeck,T., Karpova,E., Rozhdestvensky,T.S. and Brosius,J. (2007) Deletion of the MBII-85 snoRNA gene cluster in mice results in postnatal growth retardation. *PLos Genet.*, **3**, e235.
107. Qi,Y., Purtell,L., Fu,M., Lee,N.J., Aepler,J., Zhang,L., Loh,K., Enriquez,R.F., Baldock,P.A., Zolotukhin,S. *et al.* (2016) Snord116 is critical in the regulation of food intake and body weight. *Sci. Rep.*, **6**, 18614.
108. Qi,Y., Purtell,L., Fu,M., Zhang,L., Zolotukhin,S., Campbell,L. and Herzog,H. (2017) Hypothalamus specific re-introduction of SNORD116 into otherwise Snord116 deficient mice increased energy expenditure. *J. Neuroendocrinol.*, **29**, e12457.
109. Polex-Wolf,J., Lam,B.Y., Larder,R., Tadross,J., Rimmington,D., Bosch,F., Cenzano,V.J., Ayuso,E., Ma,M.K., Rainbow,K. *et al.* (2018) Hypothalamic loss of Snord116 recapitulates the hyperphagia of Prader-Willi syndrome. *J. Clin. Invest.*, **128**, 960–969.
110. Purtell,L., Qi,Y., Campbell,L., Sainsbury,A. and Herzog,H. (2017) Adult-onset deletion of the Prader-Willi syndrome susceptibility gene Snord116 in mice results in reduced feeding and increased fat mass. *Transl Pediatr*, **6**, 88–97.
111. Zhang,Q., Bouma,G.J., McClellan,K. and Tobet,S. (2012) Hypothalamic expression of snoRNA Snord116 is consistent with a link to the hyperphagia and obesity symptoms of Prader-Willi syndrome. *Int. J. Dev. Neurosci.*, **30**, 479–485.
112. Doe,C.M., Relkovic,D., Garfield,A.S., Dalley,J.W., Theobald,D.E., Humby,T., Wilkinson,L.S. and Isles,A.R. (2009) Loss of the imprinted snoRNA mbii-52 leads to increased 5htr2c pre-RNA editing and altered 5HT2CR-mediated behaviour. *Hum. Mol. Genet.*, **18**, 2140–2148.
113. Garfield,A.S., Davies,J.R., Burke,L.K., Furby,H.V., Wilkinson,L.S., Heisler,L.K. and Isles,A.R. (2016) Increased alternate splicing of Htr2c in a mouse model for Prader-Willi syndrome leads disruption of 5HT2C receptor mediated appetite. *Mol. Brain*, **9**, 95.
114. Stefan,M., Ji,H., Simmons,R.A., Cummings,D.E., Ahima,R.S., Friedman,M.I. and Nicholls,R.D. (2005) Hormonal and metabolic defects in a Prader-Willi syndrome mouse model with neonatal failure to thrive. *Endocrinology*, **146**, 4377–4385.
115. Bennett,J.A., Germani,T., Haqq,A.M. and Zwaigenbaum,L. (2015) Autism spectrum disorder in Prader-Willi syndrome: a systematic review. *Am. J. Med. Genet. A*, **167A**, 2936–2944.
116. Lee,C., Kang,E.Y., Gandal,M.J., Eskin,E. and Geschwind,D.H. (2019) Profiling allele-specific gene expression in brains from individuals with autism spectrum disorder reveals preferential minor allele usage. *Nat. Neurosci.*, **22**, 1521–1532.
117. Yin,Q.F., Yang,L., Zhang,Y., Xiang,J.F., Wu,Y.W., Carmichael,G.G. and Chen,L.L. (2012) Long noncoding RNAs with snoRNA ends. *Mol. Cell*, **48**, 219–230.
118. Zhang,X.O., Yin,Q.F., Wang,H.B., Zhang,Y., Chen,T., Zheng,P., Lu,X., Chen,L.L. and Yang,L. (2014) Species-specific alternative splicing leads to unique expression of sno-lncRNAs. *BMC Genomics*, **15**, 287.
119. Olsen,B.N., Schlesinger,P.H., Ory,D.S. and Baker,N.A. (2012) Side-chain oxysterols: from cells to membranes to molecules. *Biochim. Biophys. Acta*, **1818**, 330–336.
120. Brandis,K.A., Gale,S., Jinn,S., Langmade,S.J., Dudley-Rucker,N., Jiang,H., Sidhu,R., Ren,A., Goldberg,A., Schaffer,J.E. *et al.* (2013) Box C/D small nucleolar RNA (snoRNA) U60 regulates intracellular cholesterol trafficking. *J. Biol. Chem.*, **288**, 35703–35713.
121. Jinn,S., Brandis,K.A., Ren,A., Chacko,A., Dudley-Rucker,N., Gale,S.E., Sidhu,R., Fujiwara,H., Jiang,H., Olsen,B.N. *et al.* (2015) snoRNA U17 regulates cellular cholesterol trafficking. *Cell Metab.*, **21**, 855–867.
122. Reed,B.D., Charos,A.E., Szekely,A.M., Weissman,S.M. and Snyder,M. (2008) Genome-wide occupancy of SREBP1 and its partners NFY and SP1 reveals novel functional roles and combinatorial regulation of distinct classes of genes. *PLoS Genet.*, **4**, e1000133.
123. Ly,L.D., Xu,S., Choi,S.K., Ha,C.M., Thoudam,T., Cha,S.K., Wiederkehr,A., Wollheim,C.B., Lee,I.K. and Park,K.S. (2017) Oxidative stress and calcium dysregulation by palmitate in type 2 diabetes. *Exp. Mol. Med.*, **49**, e291.
124. Michel,C.I., Holley,C.L., Scruggs,B.S., Sidhu,R., Brookheart,R.T., Listenberger,L.L., Behlke,M.A., Ory,D.S. and Schaffer,J.E. (2011) Small nucleolar RNAs U32a, U33, and U35a are critical mediators of metabolic stress. *Cell Metab.*, **14**, 33–44.
125. Lee,J., Harris,A.N., Holley,C.L., Mahadevan,J., Pyles,K.D., Lavagnino,Z., Scherrer,D.E., Fujiwara,H., Sidhu,R., Zhang,J. *et al.* (2016) Rpl13a small nucleolar RNAs regulate systemic glucose metabolism. *J. Clin. Invest.*, **126**, 4616–4625.
126. Wiederkehr,A. and Wollheim,C.B. (2012) Mitochondrial signals drive insulin secretion in the pancreatic beta-cell. *Mol. Cell Endocrinol.*, **353**, 128–137.
127. Elliott,B.A., Ho,H.T., Ranganathan,S.V., Vangaveti,S., Ilkayeva,O., Abou Assi,H., Choi,A.K., Agris,P.F. and Holley,C.L. (2019) Modification of messenger RNA by 2′-O-methylation regulates gene expression *in vivo*. *Nat. Commun.*, **10**, 3401.
128. Colon,S., Page-McCaw,P. and Bhave,G. (2017) Role of hypohalous acids in basement membrane homeostasis. *Antioxid Redox Signal*, **27**, 839–854.
129. Mazumder,B., Sampath,P., Seshadri,V., Maitra,R.K., DiCorleto,P.E. and Fox,P.L. (2003) Regulated release of L13a from the 60S ribosomal subunit as a mechanism of transcript-specific translational control. *Cell*, **115**, 187–198.
130. Poddar,D., Basu,A., Baldwin,W.M. 3rd, Kondratov,R.V., Barik,S. and Mazumder,B. (2013) An extraribosomal function of ribosomal protein L13a in macrophages resolves inflammation. *J. Immunol.*, **190**, 3600–3612.
131. Scruggs,B.S., Michel,C.I., Ory,D.S. and Schaffer,J.E. (2012) SmD3 regulates intronic noncoding RNA biogenesis. *Mol. Cell Biol.*, **32**, 4092–4103.
132. Holley,C.L., Li,M.W., Scruggs,B.S., Matkovich,S.J., Ory,D.S. and Schaffer,J.E. (2015) Cytosolic accumulation of small nucleolar RNAs (snoRNAs) is dynamically regulated by NADPH oxidase. *J. Biol. Chem.*, **290**, 11741–11748.
133. Rimer,J.M., Lee,J., Holley,C.L., Crowder,R.J., Chen,D.L., Hanson,P.I., Ory,D.S. and Schaffer,J.E. (2018) Long-range function of secreted small nucleolar RNAs that direct 2′-O-methylation. *J. Biol. Chem.*, **293**, 13284–13296.
134. Rogelj,B., Hartmann,C.E., Yeo,C.H., Hunt,S.P. and Giese,K.P. (2003) Contextual fear conditioning regulates the expression of brain-specific small nucleolar RNAs in hippocampus. *Eur. J. Neurosci.*, **18**, 3089–3096.
135. Lee,A.R., Kim,J.H., Cho,E., Kim,M. and Park,M. (2017) Dorsal and ventral hippocampus differentiate in functional pathways and differentially associate with neurological disease-related genes during postnatal development. *Front. Mol. Neurosci.*, **10**, 331.

136. Li,D., Zhang,J., Wang,M., Li,X., Gong,H., Tang,H., Chen,L., Wan,L. and Liu,Q. (2018) Activity dependent LoNA regulates translation by coordinating rRNA transcription and methylation. *Nat. Commun.*, **9**, 1726.
137. Galiveti,C.R., Rozhdestvensky,T.S., Brosius,J., Lehrach,H. and Konthur,Z. (2010) Application of housekeeping npcRNAs for quantitative expression analysis of human transcriptome by real-time PCR. *RNA*, **16**, 450–461.
138. Bohnsack,M.T., Kos,M. and Tollervey,D. (2008) Quantitative analysis of snoRNA association with pre-ribosomes and release of snR30 by Rok1 helicase. *EMBO Rep.*, **9**, 1230–1236.
139. Raabe,C.A., Tang,T.H., Brosius,J. and Rozhdestvensky,T.S. (2014) Biases in small RNA deep sequencing data. *Nucleic Acids Res.*, **42**, 1414–1426.
140. Bazeley,P.S., Shepelev,V., Talebizadeh,Z., Butler,M.G., Fedorova,L., Filatov,V. and Fedorov,A. (2008) snoTARGET shows that human orphan snoRNA targets locate close to alternative splice junctions. *Gene*, **408**, 172–179.
141. Tafer,H., Kehr,S., Hertel,J., Hofacker,I.L. and Stadler,P.F. (2010) RNAsnoop: efficient target prediction for H/ACA snoRNAs. *Bioinformatics*, **26**, 610–616.
142. Kehr,S., Bartschat,S., Stadler,P.F. and Tafer,H. (2011) PLEXY: efficient target prediction for box C/D snoRNAs. *Bioinformatics*, **27**, 279–280.
143. van Nues,R.W., Granneman,S., Kudla,G., Sloan,K.E., Chicken,M., Tollervey,D. and Watkins,N.J. (2011) Box C/D snoRNP catalysed methylation is aided by additional pre-rRNA base-pairing. *EMBO J.*, **30**, 2420–2430.
144. Ideue,T., Hino,K., Kitao,S., Yokoi,T. and Hirose,T. (2009) Efficient oligonucleotide-mediated degradation of nuclear noncoding RNAs in mammalian cultured cells. *RNA*, **15**, 1578–1587.
145. Liang,X.H., Vickers,T.A., Guo,S. and Crooke,S.T. (2011) Efficient and specific knockdown of small non-coding RNAs in mammalian cells and in mice. *Nucleic Acids Res.*, **39**, e13.
146. Coulson,R.L., Powell,W.T., Yasui,D.H., Dileep,G., Resnick,J. and LaSalle,J.M. (2018) Prader-Willi locus Snord116 RNA processing requires an active endogenous allele and neuron-specific splicing by Rbfox3/NeuN. *Hum. Mol. Genet.*, **27**, 4051–4060.
147. Maden,B.E. (2001) Mapping 2′-O-methyl groups in ribosomal RNA. *Methods*, **25**, 374–382.
148. Bakin,A. and Ofengand,J. (1993) Four newly located pseudouridylate residues in Escherichia coli 23S ribosomal RNA are all at the peptidyltransferase center: analysis by the application of a new sequencing technique. *Biochemistry*, **32**, 9754–9762.
149. Schwartz,S., Bernstein,D.A., Mumbach,M.R., Jovanovic,M., Herbst,R.H., Leon-Ricardo,B.X., Engreitz,J.M., Guttman,M., Satija,R., Lander,E.S. *et al.* (2014) Transcriptome-wide mapping reveals widespread dynamic-regulated pseudouridylation of ncRNA and mRNA. *Cell*, **159**, 148–162.
150. Birkedal,U., Christensen-Dalsgaard,M., Krogh,N., Sabarinathan,R., Gorodkin,J. and Nielsen,H. (2015) Profiling of ribose methylations in RNA by high-throughput sequencing. *Angew. Chem. Int. Ed. Engl.*, **54**, 451–455.
151. Marchand,V., Blanloeil-Oillo,F., Helm,M. and Motorin,Y. (2016) Illumina-based RiboMethSeq approach for mapping of 2′-O-Me residues in RNA. *Nucleic Acids Res.*, **44**, e135.
152. Gumienny,R., Jedlinski,D.J., Schmidt,A., Gypas,F., Martin,G., Vina-Vilaseca,A. and Zavolan,M. (2017) High-throughput identification of C/D box snoRNA targets with CLIP and RiboMeth-seq. *Nucleic Acids Res.*, **45**, 2341–2353.
153. Yamauchi,Y., Nobe,Y., Izumikawa,K., Higo,D., Yamagishi,Y., Takahashi,N., Nakayama,H., Isobe,T. and Taoka,M. (2016) A mass spectrometry-based method for direct determination of pseudouridine in RNA. *Nucleic Acids Res.*, **44**, e59.
154. Taoka,M., Nobe,Y., Hori,M., Takeuchi,A., Masaki,S., Yamauchi,Y., Nakayama,H., Takahashi,N. and Isobe,T. (2015) A mass spectrometry-based method for comprehensive quantitative determination of post-transcriptional RNA modifications: the complete chemical structure of Schizosaccharomyces pombe ribosomal RNAs. *Nucleic Acids Res.*, **43**, e115.
155. Lacoux,C., Di Marino,D., Boyl,P.P., Zalfa,F., Yan,B., Ciotti,M.T., Falconi,M., Urlaub,H., Achsel,T., Mougin,A. *et al.* (2012) BC1-FMRP interaction is modulated by 2′-O-methylation: RNA-binding activity of the tudor domain and translational regulation at synapses. *Nucleic Acids Res.*, **40**, 4086–4096.
156. Rozhdestvensky,T.S., Crain,P.F. and Brosius,J. (2007) Isolation and posttranscriptional modification analysis of native BC1 RNA from mouse brain. *RNA Biol.*, **4**, 11–15.
157. Engreitz,J.M., Pandya-Jones,A., McDonel,P., Shishkin,A., Sirokman,K., Surka,C., Kadri,S., Xing,J., Goren,A., Lander,E.S. *et al.* (2013) The Xist lncRNA exploits three-dimensional genome architecture to spread across the X chromosome. *Science*, **341**, 1237973.
158. McHugh,C.A., Chen,C.K., Chow,A., Surka,C.F., Tran,C., McDonel,P., Pandya-Jones,A., Blanco,M., Burghard,C., Moradian,A. *et al.* (2015) The Xist lncRNA interacts directly with SHARP to silence transcription through HDAC3. *Nature*, **521**, 232–236.
159. Riley,K.J. and Steitz,J.A. (2013) The "Observer Effect" in genome-wide surveys of protein-RNA interactions. *Mol. Cell*, **49**, 601–604.
160. Ule,J., Jensen,K.B., Ruggiu,M., Mele,A., Ule,A. and Darnell,R.B. (2003) CLIP identifies Nova-regulated RNA networks in the brain. *Science*, **302**, 1212–1215.
161. Licatalosi,D.D., Mele,A., Fak,J.J., Ule,J., Kayikci,M., Chi,S.W., Clark,T.A., Schweitzer,A.C., Blume,J.E., Wang,X. *et al.* (2008) HITS-CLIP yields genome-wide insights into brain alternative RNA processing. *Nature*, **456**, 464–469.
162. Bohnsack,M.T., Tollervey,D. and Granneman,S. (2012) Identification of RNA helicase target sites by UV cross-linking and analysis of cDNA. *Methods Enzymol.*, **511**, 275–288.
163. Granneman,S., Kudla,G., Petfalski,E. and Tollervey,D. (2009) Identification of protein binding sites on U3 snoRNA and pre-rRNA by UV cross-linking and high-throughput analysis of cDNAs. *Proc. Natl. Acad. Sci. U.S.A.*, **106**, 9613–9618.
164. Hafner,M., Landthaler,M., Burger,L., Khorshid,M., Hausser,J., Berninger,P., Rothballer,A., Ascano,M. Jr., Jungkamp,A.C., Munschauer,M. *et al.* (2010) Transcriptome-wide identification of RNA-binding protein and microRNA target sites by PAR-CLIP. *Cell*, **141**, 129–141.
165. Youssef,O.A., Safran,S.A., Nakamura,T., Nix,D.A., Hotamisligil,G.S. and Bass,B.L. (2015) Potential role for snoRNAs in PKR activation during metabolic stress. *Proc. Natl. Acad. Sci. U.S.A.*, **112**, 5023–5028.
166. Huppertz,I., Attig,J., D'Ambrogio,A., Easton,L.E., Sibley,C.R., Sugimoto,Y., Tajnik,M., Konig,J. and Ule,J. (2014) iCLIP: protein-RNA interactions at nucleotide resolution. *Methods*, **65**, 274–287.
167. Engreitz,J.M., Sirokman,K., McDonel,P., Shishkin,A.A., Surka,C., Russell,P., Grossman,S.R., Chow,A.Y., Guttman,M. and Lander,E.S. (2014) RNA-RNA interactions enable specific targeting of noncoding RNAs to nascent Pre-mRNAs and chromatin sites. *Cell*, **159**, 188–199.
168. Grosswendt,S., Filipchyk,A., Manzano,M., Klironomos,F., Schilling,M., Herzog,M., Gottwein,E. and Rajewsky,N. (2014) Unambiguous identification of miRNA:target site interactions by different types of ligation reactions. *Mol. Cell*, **54**, 1042–1054.
169. Kudla,G., Granneman,S., Hahn,D., Beggs,J.D. and Tollervey,D. (2011) Cross-linking, ligation, and sequencing of hybrids reveals RNA-RNA interactions in yeast. *Proc. Natl. Acad. Sci. U.S.A.*, **108**, 10010–10015.
170. Helwak,A. and Tollervey,D. (2014) Mapping the miRNA interactome by cross-linking ligation and sequencing of hybrids (CLASH). *Nat. Protoc.*, **9**, 711–728.
171. Sugimoto,Y., Vigilante,A., Darbo,E., Zirra,A., Militti,C., D'Ambrogio,A., Luscombe,N.M. and Ule,J. (2015) hiCLIP reveals the *in vivo* atlas of mRNA secondary structures recognized by Staufen 1. *Nature*, **519**, 491–494.
172. Sugimoto,Y., Chakrabarti,A.M., Luscombe,N.M. and Ule,J. (2017) Using hiCLIP to identify RNA duplexes that interact with a specific RNA-binding protein. *Nat. Protoc.*, **12**, 611–637.
173. Lu,Z., Gong,J. and Zhang,Q.C. (2018) PARIS: psoralen analysis of RNA interactions and structures with high throughput and resolution. *Methods Mol. Biol.*, **1649**, 59–84.
174. Aw,J.G., Shen,Y., Wilm,A., Sun,M., Lim,X.N., Boon,K.L., Tapsin,S., Chan,Y.S., Tan,C.P., Sim,A.Y. *et al.* (2016) *In vivo*

mapping of eukaryotic RNA interactomes reveals principles of higher-order organization and regulation. *Mol. Cell*, **62**, 603–617.
175. Ziv,O., Gabryelska,M.M., Lun,A.T.L., Gebert,L.F.R., Sheu-Gruttadauria,J., Meredith,L.W., Liu,Z.Y., Kwok,C.K., Qin,C.F., MacRae,I.J. *et al.* (2018) COMRADES determines *in vivo* RNA structures and interactions. *Nat. Methods*, **15**, 785–788.
176. Bao,X., Zhu,X., Liao,B., Benda,C., Zhuang,Q., Pei,D., Qin,B. and Esteban,M.A. (2013) MicroRNAs in somatic cell reprogramming. *Curr. Opin. Cell Biol.*, **25**, 208–214.
177. Spitalieri,P., Talarico,V.R., Murdocca,M., Novelli,G. and Sangiuolo,F. (2016) Human induced pluripotent stem cells for monogenic disease modelling and therapy. *World J. Stem Cells*, **8**, 118–135.
178. Burnett,L.C., LeDuc,C.A., Sulsona,C.R., Paull,D., Eddiry,S., Levy,B., Salles,J.P., Tauber,M., Driscoll,D.J., Egli,D. *et al.* (2016) Induced pluripotent stem cells (iPSC) created from skin fibroblasts of patients with Prader-Willi syndrome (PWS) retain the molecular signature of PWS. *Stem Cell Res.*, **17**, 526–530.
179. Yang,J., Cai,J., Zhang,Y., Wang,X., Li,W., Xu,J., Li,F., Guo,X., Deng,K., Zhong,M. *et al.* (2010) Induced pluripotent stem cells can be used to model the genomic imprinting disorder Prader-Willi syndrome. *J. Biol. Chem.*, **285**, 40303–40311.
180. Chamberlain,S.J., Chen,P.F., Ng,K.Y., Bourgois-Rocha,F., Lemtiri-Chlieh,F., Levine,E.S. and Lalande,M. (2010) Induced pluripotent stem cell models of the genomic imprinting disorders Angelman and Prader-Willi syndromes. *Proc. Natl. Acad. Sci. U.S.A.*, **107**, 17668–17673.
181. Agarwal,S., Loh,Y.H., McLoughlin,E.M., Huang,J., Park,I.H., Miller,J.D., Huo,H., Okuka,M., Dos Reis,R.M., Loewer,S. *et al.* (2010) Telomere elongation in induced pluripotent stem cells from dyskeratosis congenita patients. *Nature*, **464**, 292–296.
182. Batista,L.F., Pech,M.F., Zhong,F.L., Nguyen,H.N., Xie,K.T., Zaug,A.J., Crary,S.M., Choi,J., Sebastiano,V., Cherry,A. *et al.* (2011) Telomere shortening and loss of self-renewal in dyskeratosis congenita induced pluripotent stem cells. *Nature*, **474**, 399–402.
183. MacNeil,D.E., Lambert-Lanteigne,P. and Autexier,C. (2019) N-terminal residues of human dyskerin are required for interactions with telomerase RNA that prevent RNA degradation. *Nucleic Acids Res.*, **47**, 5368–5380.
184. Xu,H., Yao,J., Wu,D.C. and Lambowitz,A.M. (2019) Improved TGIRT-seq methods for comprehensive transcriptome profiling with decreased adapter dimer formation and bias correction. *Sci. Rep.*, **9**, 7953.
185. Birnbaum,K.D. (2018) Power in numbers: Single-cell RNA-seq strategies to dissect complex tissues. *Annu. Rev. Genet.*, **52**, 203–221.
186. Chen,G., Ning,B. and Shi,T. (2019) Single-sell RNA-seq technologies and related computational data analysis. *Front. Genet.*, **10**, 317.
187. Luecken,M.D. and Theis,F.J. (2019) Current best practices in single-cell RNA-seq analysis: a tutorial. *Mol Syst Biol.*, **15**, e8746.
188. Stoeckius,M., Hafemeister,C., Stephenson,W., Houck-Loomis,B., Chattopadhyay,P.K., Swerdlow,H., Satija,R. and Smibert,P. (2017) Simultaneous epitope and transcriptome measurement in single cells. *Nat. Methods*, **14**, 865–868.
189. Incarnato,D. and Oliviero,S. (2017) The RNA epistructurome: Uncovering RNA function by studying structure and post-transcriptional modifications. *Trends Biotechnol.*, **35**, 318–333.
190. Incarnato,D., Morandi,E., Simon,L.M. and Oliviero,S. (2018) RNA Framework: an all-in-one toolkit for the analysis of RNA structures and post-transcriptional modifications. *Nucleic Acids Res.*, **46**, e97.